Published in final edited form as:
J Immunol. 2013 September 1; 191(5): . doi:10.4049/jimmunol.1203268.

Two phases of inflammatory mediator production defined by the study of IRAK2 and IRAK1 knock-in mice

Eduardo Pauls[#*,†], **Sambit K. Nanda**[#*], **Hilary Smith**[*], **Rachel Toth**[*], **J. Simon C. Arthur**[*,‡], and **Philip Cohen**[*]

[*]Medical Research Council Protein Phosphorylation and Ubiquitylation Unit, Sir James Black Centre, University of Dundee, Dundee DD1 5EH, United Kingdom

[†]IrsiCaixa, Hospital Germans Trias i Pujol, Universitat Autònoma de Barcelona, Badalona 08916, Spain

[‡]Division of Cell Signaling and Immunology Unit, Sir James Black Centre, University of Dundee, DD1 5EH, United Kingdom

[#] These authors contributed equally to this work.

Abstract

The roles of IL-1R-associated kinase (IRAK)2 and IRAK1 in cytokine production were investigated using immune cells from knock-in mice expressing the TNFR-associated factor 6 (TRAF6) binding-defective mutant IRAK2[E525A] or the catalytically inactive IRAK1[D359A] mutant. In bone marrow-derived macrophages (BMDMs), the IRAK2-TRAF6 interaction was required for the late (2-8 h) but not the early phase (0-2 h) of *il6, and tnfa* mRNA production and hence for IL-6 and TNF-α secretion by TLR agonists that signal via MyD88. Loss of the IRAK2-TRAF6 interaction had little effect on the MyD88-dependent production of anti-inflammatory molecules produced during the early phase, such as Dual Specificity Phosphatase 1, and a modest effect on IL-10 secretion. The LPS/TLR4-stimulated production of *il6* and *tnfa* mRNA and IL-6 and TNF-α secretion was hardly affected, because the Toll/IL-1R domain-containing adapter-inducing IFN-β (TRIF) signaling pathway was used instead of the IRAK2-TRAF6 interaction to sustain late-phase mRNA production. IRAK1 catalytic activity was not rate-limiting for *il6, tnfa or il10* mRNA production or the secretion of these cytokines by BMDMs, but IFN-β mRNA induction by TLR7 and TLR9 agonists was greatly delayed in plasmacytoid dendritic cells (pDCs) from IRAK1[D359A] mice. In contrast, IFN-β mRNA production was little affected in pDCs from IRAK2[E525A] mice, but subsequent IFN-α mRNA production and IFN-α secretion were reduced. IFN-β and IFN-α production were abolished in pDCs from IRAK1[D359A] ×IRAK2[E525A] double knock-in mice. Our results establish that the IRAK2-TRAF6 interaction is rate limiting for the late, but not the early phase of cytokine production in BMDM and pDCs, and that the IRAK2-TRAF6 interaction is needed to sustain IκB-inducing kinase β activity during prolonged activation of the MyD88 signalling network.

Introduction

Nearly all TLRs signal via the adaptor MyD88, except for TLR3, which signals via the adaptor Toll/IL-1R domain-containing adapter-inducing IFN-β (TRIF) (1, 2), and TLR4, which uniquely signals via both MyD88 and TRIF (3). How the TLR-MyD88 interaction

Correspondence to: Philip Cohen.

Corresponding author: Dr. Philip Cohen, Medical Research Council Protein Phosphorylation Unit, The Sir James Black Centre, University of Dundee, Dow Street, Dundee, DD1 5EH, United Kingdom p.cohen@dundee.ac.uk.

Europe PMC Funders Author Manuscripts

drives inflammatory mediator production at the molecular level is therefore central to our understanding of innate immunity. It is well established that the formation of the agonist-TLR-MyD88 complex is followed by the recruitment and oligomerization of IL-1R-associated kinase 4 (IRAK4). The death domain (DD) of IRAK4 then interacts with the DD of IRAK1 and IRAK2 to form a structure termed the "Myddosome" (4, 5). IRAK1 and IRAK2 undergo covalent modification by phosphorylation and ubiquitylation, and interact with TNFR-associated factor 6 (TRAF6) via their C-terminal TRAF-binding domains (6). This increases the E3 ubiquitin ligase activity of TRAF6, which is thought to produce Lys63-linked polyubiquitin chains in the presence of UBE1 and the E2 conjugating complex Ubc13-Uev1a. Lys^{63}-linked polyubiquitin chains can interact with the TGFβ-activated kinase (TAK1) binding protein (TAB) 2 and TAB3 components of the TAK1 complex, which has been suggested to induce a conformational change that leads to the auto-activation of TAK1 (7, 8). TAK1 can then initiate the activation of the MAPK kinases that switch on p38 MAPK and JNKs. TAK1 may also initiate the activation of IκB-inducing kinase α (IKKα) and IKKβ provided that linear polyubiquitin chains produced by the E3 ubiquitin ligase linear ubiquitin assembly complex are bound to NEMO (9, 10), which is an essential regulatory component of the canonical IKK complex. Together, the canonical IKKs and MAPKs, and other protein kinases that they activate, catalyze many phosphorylation events that stimulate transcriptional and post-transcriptional events that culminate in the production of inflammatory mediators. For example, IKKβ not only induces the activation of the transcription factor NF-κB, but also activates the protein kinase Tpl2 (11, 12), which leads to the activation of the MAPKs ERK1 and ERK2 (13).

Much of our knowledge about the physiological roles of IRAK1 and IRAK2 has been obtained by studying knock-out mice. Studies with macrophages from mice deficient in either IRAK1 or IRAK2 showed that they produced reduced amounts of the mRNAs encoding a number of pro-inflammatory cytokines after stimulation with the TLR2 agonist macrophage-activating lipopeptide 2 (MALP2), but mRNA production was impaired much more severely in macrophages from double knock-out mice that do not express either of these proteins (14). Consistent with these findings, IRAK1-deficient mice (15) and IRAK2-deficient mice (14, 16) were found to be more resistant to septic shock than wild type (WT) mice, whereas the double knock-out mice were far more resistant. Taken together, these results indicated that IRAK1 and IRAK2 are both required for maximal production of pro-inflammatory cytokine mRNAs. However, a much more drastic reduction in the secretion of pro-inflammatory cytokines was observed in macrophages from IRAK2-deficient mice than from IRAK1-deficient mice (14).

Plasmacytoid dendritic cells (pDCs) are a subset of dendritic cells (DCs), which produce high levels of type 1 IFNs in response to viral nucleic acids that activate TLR7 and TLR9, probably because they express high levels of IFN regulatory factor 7 constitutively (17). The production of type 1 IFNs by these cells plays an important role in defense against viral infection (reviewed (18)), but because TLR7 and TLR9 have the potential to trigger immune responses if they are recognized by immune complexes consisting of autoantibodies bound to self-RNA and self-DNA (19) they may also contribute to the development of autoimmune diseases, such as systemic lupus erythematosus (20). TLR7 and TLR9 signal via MyD88 and IKKα and IKKβ are both required for the production of type 1 IFNs by pDCs and conventional DCs (21, 22). However, in these pathways, IKKα and IKKβ exert their effects by mechanisms that are at least partially independent of NF-κB (23, 24). Interestingly, the TLR7/TLR9-stimulated production of IFN-α by pDCs was reported to be greatly impaired in IRAK1-deficient mice (25), but enhanced in pDCs from IRAK2-deficient mice (26). Based on the latter observation it was suggested that IRAK2 may function as a negative regulator of IFN-α production in these cells (26).

IRAK1 and IRAK2 are both multi-domain proteins, the DD being followed by a region rich in proline, serine and threonine residues, then the kinase domain and finally the C-terminal TRAF6 interacting domain (6, 27). Although IRAK1, like IRAK4, is catalytically active, the physiological roles of the protein kinase activity of IRAK1 are poorly understood. On the other hand, the kinase-like domain of IRAK2 lacks amino acid residues that are essential for catalysis by most protein kinases and, when expressed in and purified from transfected mammalian cells, it displays negligible kinase catalytic activity in vitro (28). It was therefore assumed IRAK2 is an inactive “pseudokinase”, one of some 40 “pseudokinases” encoded by the human genome. However, subsequently, IRAK2 was reported to undergo phosphorylation when it was immunoprecipitated from the extracts of MALP2-stimulated WT macrophages and incubated with Mg-ATP. Because this did not occur when IRAK2 was immunoprecipitated from IRAK4-deficient macrophages, it was suggested that IRAK2 was catalytically active and able to undergo autophosphorylation after it had been phosphorylated by IRAK4 (14). However, since IRAK2 and IRAK4 interact via their DD, the possibility that the protein kinase activity associated with IRAK2 immunoprecipitates was IRAK4, or another protein kinase whose activity was dependent on IRAK4 expression, was not excluded by these studies (14). Therefore, whether IRAK2 is catalytically active is still an unresolved issue.

The gene encoding IRAK2 can create four different splice variants, termed IRAK2a, IRAK2b, IRAK2c and IRAK2d (29). IRAK2a and IRAK2b both possess the DD, the pseudokinase domain and TRAF6-binding motifs and were reported to potentiate LPS-stimulated NF-κB-dependent gene expression in overexpression studies. In contrast, IRAK2c and IRAK2d lack the DD and are presumably unable to interact with IRAK4. Moreover, they inhibited NF-κB-dependent gene transcription in overexpression experiments, suggesting a potential role in the feedback control of the MyD88 signalling network (29). The IRAK2c variant was not expressed in the wild-derived mouse strain MOLF/Ei, which might explain why this mouse line produced higher levels of IL-6 in response to TLR agonists compared to the inbred strain C57BL/6J (30).

A full understanding of the physiological roles played by each IRAK family member in the MyD88 signalling network requires knowledge of the separate roles of each functional domain. This cannot be evaluated by studying cells from knock-out mice because the observed phenotypes may arise from the loss of any or all of the functional domains. In addition, ablating the expression of one IRAK family member may affect the way in which other IRAK family members interact and signal within the Myddosome. One approach to address this complex problem is to study knock-in mice carrying mutations that inactivate a single functional domain of each protein. In this paper, we investigated how the MyD88 signaling network is affected in bone marrow-derived macrophages (BMDMs) and pDCs from knock-in mice that express the catalytically inactive mutant IRAK1[D359A] instead of the WT protein and in knock-in mice that express IRAK2[E525A], a mutant that is unable to interact with TRAF6. These and other experiments have revealed that the IRAK2-TRAF6 interaction is needed to sustain IKKβ activity during prolonged TLR stimulation, and we show that this is critical for the late surge in *il6* and *tnfa* mRNA production in BMDMs, and for IRAK2 to stimulate IFN-α production by TLR9 agonists by pDCs. In contrast, IRAK1 catalytic activity is critical for type I IFN production by pDCs, but is not rate limiting for the production of *il6* and *tnfa* mRNA by BMDMs.

Material and Methods

Materials

The TLR agonists Pam_3CSK_4, lipoteichoic acid (LTA), R848 (also called Imiquimod) CpG type B (ODN1826) and CpG type A (ODN1585) were from Invivogen, LPS (*E. coli*

O55:B5) from Alexis Biochemicals and the TLR7 agonist poly(deoxyuridylic acid) [poly(dU)] was from Sigma-Aldrich. The poly(dU) was added to the culture medium conjugated with Lipofectamine 2000 (Invitrogen) (23). The phage λ phosphatase was purchased from New England Biolabs and ubiquitin-specific protease 2 (USP2) was provided by Dr Axel Knebel, Medical Research Council Protein Phosphorylation and Ubiquitylation Unit. Actinomycin D was purchased from Sigma. BI605906 (31) was synthesized by Dr Natalia Shpiro, Medical Research Council Protein Phosphorylation and Ubiquitylation Unit.

Antibodies

Antibodies that recognize IKKα phosphorylated at Ser^{176} and Ser^{180} and IKKβ phosphorylated at Ser^{177} and Ser^{181}, p105/NF-κB1 phosphorylated at Ser^{933}, p38 MAPK phosphorylated at the TGY motif, ERK1/ERK2 phosphorylated at the TEY motif, antibodies that recognize all forms of ERK1/ERK2, JNK1/2 and p38α MAPK, as well as antibodies that recognize IRAK1 (clone number D51G7), antibodies that recognize all forms of STAT1 or STAT1 phosphorylated at Tyr^{701} were from Cell Signaling Technology. An antibody recognizing JNK phosphorylated at the TPY motif was obtained from Invitrogen, anti-TRAF6 for immunoblotting from Santa Cruz, and anti-α-tubulin from Sigma. A rabbit polyclonal antibody for immunoblotting of mouse IRAK2 (raised against a C-terminal peptide that is common to all four spliced variants of mouse IRAK2) was purchased from Abcam, whereas a rabbit secondary antibody conjugated to HRP was from Pierce. The HRP-conjugated anti-HA antibody was from Roche, and HRP-conjugated anti-FLAG antibody was from Sigma. Antibodies against human IRAK2 (sheep number S479C, third bleed), mouse IRAK1 (sheep number S690C, third bleed) and TRAF6 (sheep number S691C, third bleed) for immunoprecipitation experiments were produced by the Antibody Production Team of the Division of Signal Transduction Therapy, Medical Research Council Protein Phosphorylation Unit, University of Dundee, coordinated by Dr James Hastie.

Generation of IRAK2[E525A] knock-in mice

To generate knock-in mice expressing the IRAK2[E525A] mutant (numbering refers to the IRAK2a variant) instead of the WT protein, we mutated the GAA codon for Glu at this position to the GCA codon for Ala. Glu^{525} is encoded in exon 12 of the mouse *Irak2* gene, and a targeting vector was constructed to introduce the required mutation. This vector was designed to introduce loxP sites on either side of exon 12 in addition to mutating Glu^{525} to Ala. Neomycin and thymidine kinase cassettes were included to allow for positive and negative selection, respectively, in the embryonic stem (ES) cells. The neomycin marker consisted of a pGK promoter, the neomycin-resistance gene open reading frame, an internal ribosome entry site sequence, an in-frame start codon and the splice donor site from exon 12 of IRAK2. This selection cassette acts as a polyA trap and also allows a reverse transcription-based RNA screen for homologous recombination. The three arms of homology to the IRAK2 locus were generated by PCR for an appropriate murine BAC clone using the primers listed in Supplementary Table I. All PCR products were fully sequenced to ensure the absence of PCR-generated mutations.

The targeting vector was used to generate mutant ES cells as described previously (32). Positive ES cells were used to generate chimeric mice via blastocyst injections. Chimeric mice giving germ-line transmission were bred to C57/Bl6 Flp*e* transgenic mice (TaconicArtemis) to excise the two selectable markers, whose deletion was confirmed by PCR screening. Routine genotyping of the mice was carried out using the same primers.

Only mice that had been backcrossed at least six times were used for the experiments described in this study. All mice were maintained under specific pathogen-free conditions

and housed in accordance with United Kingdom and European Union law. Work was carried out under a United Kingdom Home Office license and was subject to and approved by local ethical review.

Generation of IRAK1[D359A] knock-in mice

The aspartyl residue present in the "DFG" motif of most protein kinases is essential for their activity because it interacts with the magnesium ion of the Mg-ATP complex. To check that this amino acid residue is also critical for the kinase activity of IRAK1, we mutated the aspartic acid residue at position 358 of human IRAK1 to alanine. The normal human IRAK1 underwent autophosphorylation when it was overexpressed in IL-1R cells, as shown by a decrease in its electrophoretic mobility, which could be reversed by treatment with a protein phosphatase. In contrast, the human IRAK1[D358A] mutant did not undergo this band shift and its mobility was unaffected by phosphatase treatment, demonstrating that it was indeed inactive (Supplemental Fig. 1A). The mutation of the aspartic acid residue of the "DFG" motif has also been found not to alter overall kinase conformation significantly (33). We therefore generated knock-in mice in which WT IRAK1 was replaced by the equivalent IRAK1[D359A] mutant as detailed previously (34).

Generation and culture of BMDMs

BMDMs were obtained by differentiating bone marrow obtained from the femur and tibia with M-CSF (R&D Systems) or L929 preconditioned medium as the source of M-CSF. Cells were maintained on bacterial grade plates for one week in DMEM supplemented with 10% (v/v) heat-inactivated FBS (Biosera), 2 mM L-glutamine, 100 U/ml penicillin G, 100 μg/ml streptomycin, 0.25 μg/ml amphotericin and 10 ng/ml M-CSF. When L929 preconditioned medium was used to prepare BMDM, bone marrow cells were differentiated in DMEM containing 20% L929-preconditioned medium, 10% heat-inactivated FBS, 100 U/ml penicillin, 100 μg/ml streptomycin, 1 mM sodium pyruvate, 0.2 mM 2-ME and non-essential amino acids at the concentrations recommended by the manufacturer (Life Technologies). Adherent BMDMs were then re-plated into 12-well tissue culture plates (5×10^5 cells) or 10 cm tissue culture grade plates (5×10^6 cells) using fresh culture medium. After re-plating, BMDMs were stimulated for up to 24 h with TLR agonists (see Results). Where indicated, cells were pre-treated for 1h with the IKKβ inhibitor BI605906 prior to stimulation.

Generation of Flt3-derived dendritic cells

Bone marrow cells extracted from the femur and tibia of mice were differentiated into Flt3 bone-marrow derived DCs by incubation for seven days in RPMI 1640 supplemented with 100 ng/ml recombinant Flt3-ligand (PeproTech), 10% FBS, 50 μM 2-ME, 10 mM HEPES, penicillin (100 U/ml) and streptomycin (100 μg/ml) as described previously (35). To determine the percentage of pDCs, cells were stained with B220 and PDC1 antibodies (Beckton-Dickinson) and analysed by flow cytometry. The percentage of pDCs (B220 plus $PDCA1^+$) in each experiment ranged from 40 to 60%. No significant differences were observed in the proportion of B220 and $PDCA1^+$ cells when comparing Flt3-DCs from different IRAK genotypes with cells obtained from WT mice. Flt3-DCs were stimulated with the concentrations of ligands specified in the figure legends.

Immunoblotting, immunoprecipitation and treatment with phosphatases and deubiquitylases

BMDMs or pDCs were rinsed in ice-cold PBS, lysed, and 10-20 μg of cell extract protein was subjected to SDS-PAGE, transferred to polyvinylidene fluoride membranes, and immunoblotted as described previously (36). For immunoprecipitation of endogenous

proteins, cell extracts (1.0 mg protein) were incubated for 16 h at 4°C with 2.5 μg anti-IRAK1, anti-IRAK2 or anti-TRAF6 antibodies. After mixing end over end for 60 min with protein-G agarose beads (15 μl), the agarose was collected and washed three times with cell lysis buffer containing 0.5 M NaCl. The immunoprecipitates were further washed in 1 ml of 50 mM HEPES pH 7.5, 100 mM NaCl, 1 mM $MnCl_2$, 5 mM DTT, 0.01% (w/v) Brij-35 and then resuspended in 30 μl of buffer containing the USP2 (1 μM) and/or bacteriophage λ phosphatase (4 U). After incubation for 45 min at 30°C, the reactions were terminated in SDS. After brief centrifugation to pellet the Protein G-agarose, the supernatants were subjected to SDS-PAGE and immunoblotted with the antibodies specified in the figure legends.

For immunoprecipitation of overexpressed HA- or FLAG-tagged proteins, cell extracts (0.25 - 0.50 mg protein) were incubated for 1 h at 4°C with 5 μl anti-HA agarose affinity gel or anti-FLAG M2 affinity gel (Sigma), respectively.

Measurement of cytokine concentrations

Following stimulation with ligands, the cell culture medium was removed, clarified by centrifugation for 10 min at 14000 × g and the levels ofIL-6, IL-10, TNF-α, MIP1α, and MIP1β were measured either by end-point ELISA Development Kits from PeproTech or the Bio-Plex Pro Assay multiplex system from Bio-Rad.

Measurement of IFNs

A total of 3.5×10^5 Flt3-DCs were incubated for 1 h in 96-well plates, then stimulated with 0.05 μM CpG type B or 1 μM CpG type A. A total of 25 μg/ml poly(dU) was conjugated with Lipofectamine 2000 to stimulate Flt3-DCs. After stimulation for 12 h the cell culture supernatants were collected, clarified by centrifugation, and frozen at −80 °C until IFN levels were analysed. The concentrations of IFN-α in the cell culture supernatant was measured by ELISA using the Verikine Mouse IFN-α kit (PBL IFN Source).

Quantitative real-time PCR

After stimulation with ligands, the cell culture medium was removed and total RNA extracted from cells using the RNeasy Micro kit (Qiagen). A total of 1 μg of RNA was reverse transcribed using random and oligo (dT) primers, iScript reverse transcriptase, and the accompanying reagents (BioRad or Quanta Biosciences), according to the manufacturer's instructions. PCRs were performed using the PerfeCT Syber Green Fast mix (Quanta Biosciences) in the BioRad iCycler (BioRad). The primers used for measuring mRNA encoding mouse *il6*, *tnfα*, and *il10* mRNA (37) and *ifnb*, *ifna4* and *ifna6* (23) were described previously. Normalisation and quantitation were performed using 18S RNA and the ΔΔCt method.

Expression vectors and cell transfection

Human IRAK1 (National Center for Biotechnology Information NP_001560.2) was amplified from IMAGE EST 6164719 using KOD Hot Start DNA Polymerase (Merck) and inserted into the Not1 site of pCMVHA-2. Mouse IRAK2 (National Center for Biotechnology Information NP_751893.3) was amplified from IMAGE EST 30733777 and cloned into the BamHI Not1 sites of pCMVFLAG-1. Mutations were created using the QuikChange method (Stratagene) but using KOD Hot Start DNA Polymerase. Human embryonic kidney 293 (HEK293) cells stably expressing the IL-1R, termed IL-1R cells and IRAK1-null IL-1R cells (a generous gift from Xiaoxia Li, Cleveland Clinic Foundation), were cultured in DMEM supplemented with 10% FBS, 2 mM glutamine, penicillin (100 U/ml) and streptomycin (100 μg/ml). Cell transfections were performed using Lipofectamine

2000 (Invitrogen) using 5 μg of expression vector DNA and 15 μl of transfection reagent per 10 ml of cell culture medium. However, for cotransfection of TRAF6 and IRAK2, 4.5 μg of HA-TRAF6 DNA and 0.5 μg FLAG-IRAK2 DNA were used.

Statistical analysis

Data were analysed with the PRISM statistical package and, if not stated otherwise, was distributed normally and expressed as the mean ± SEM/SD. Statistical significance was calculated using the unpaired, two-tailed, Student *t* test.

Results

Generation of IRAK2 knock-in mice

We generated knock-in mice in which WT IRAK2 was replaced by IRAK2[E525A] as described in Materials and Methods (Fig 1A). The mice were born at normal Mendelian frequencies and were of normal size and weight (results not shown). The mutant protein was expressed at similar levels to WT IRAK2 in BMDMs (Fig 1B). Both the WT and mutant forms of IRAK2 migrated as a major, more slowly migrating band of apparent molecular mass 75 kDa and a minor, more rapidly migrating component of 65 kDa. The molecular masses are consistent with the more slowly migrating band being the IRAK2a and/or IRAK2b alternatively spliced variants and the more rapidly migrating band being the IRAK2c and/or IRAK2d, variants that lack the DD (see the introduction).

Glu^{525} of murine IRAK2 is equivalent to Glu^{528} of human IRAK2, which lies in one of the two putative TRAF6-binding motifs of IRAK2 (Pro-X-Glu-X-X-A), where A is an aromatic or acidic residue (6). The mutation of Glu^{528} to Ala in human IRAK2 has been reported to prevent the activation of TRAF6 E3 ligase activity in overexpression studies (38). To investigate whether the interaction between mouse IRAK2 and mouse TRAF6 was affected, we co-transfected DNA vectors encoding tagged versions of these proteins into IRAK1-null human HEK293 cells that stably express the IL-1R, termed here IL-1R cells (39). We found that WT mouse IRAK2 interacted with TRAF6 as expected, but the mouse IRAK2[E525A] mutant did not (Fig 1C). The mouse IRAK2[E525A] mutant was also unable to interact with the endogenous human TRAF6 in IRAK1-null IL-1R cells, in contrast to WT mouse IRAK2 (Fig 1D). We further showed that, in contrast to the WT mouse IRAK2, the endogenous mouse IRAK2[E525A] mutant did not interact with the endogenous TRAF6 in extracts from R848-stimulated BMDMs from 15 min to 4 h after stimulation (Fig 1E). Thus IRAK2[E525A] is a mutation that prevents the interaction of IRAK2 and TRAF6.

Decreased MyD88-dependent activation of the canonical IKK complex and MAPKs after prolonged TLR stimulation in BMDMs from IRAK2[E525A] mice

It is well documented that the stimulation of macrophages with TLR agonists is followed by a strong activation of several MAPK cascades and the canonical IKK complex within minutes, but activation is transient and returns to much lower levels after 30-60 min of stimulation. These low levels of activation are maintained for a couple of hours before beginning to rise again. In the present study, we monitored the activation of IKKα, IKKβ and MAPKs for a prolonged period using antibodies that recognize amino acid residues whose phosphorylation is required for the activation of these protein kinases. We observed that the activation of the MAPKs JNK, p38 MAPK and ERK1/ERK2 induced by R848, a TLR7 agonist, or Pam_3CSK_4, an activator of the TLR1/2 heterodimer, were similar in BMDMs from IRAK2[E525A] and WT mice, for up to one hour after stimulation, but the activation of IKKα/β and the phosphorylation of the IKKβ substrate p105 (11, 40), was partially reduced in BMDMs from the IRAK2[E525A] mice (Figs 2A and 2B). The activation of IKKβ and the phosphorylation of p105 was virtually abolished in BMDM from

the IRAK2[E525A] knock-in mice after stimulation for 2-4 h (highlighted by the arrows in Figs 2A and 2B), and the activation of MAPKs was also partially reduced at these later times.

Phosphorylation, ubiquitylation and expression of IRAK1 and IRAK2

To investigate why IRAK2 became rate-limiting for the activation of IKKβ after prolonged stimulation, we studied the covalent modification and expression of IRAK1 and IRAK2 following stimulation with R848. The unmodified form of IRAK1 largely disappeared from the cell extracts when BMDM from WT mice was stimulated for 15 min with R848, but could be recovered by incubation with a combination of the protein phosphatase from phage λ and the deubiquitylase USP2 (Fig 2C). This demonstrated that the disappearance of unmodified IRAK1 had not resulted from its degradation, but from conversion to a variety of more slowly migrating phosphorylated and ubiquitylated species. However, after stimulation with R848 for 2 h, the unmodified form of IRAK1 could only be recovered partially by phosphatase/deubiquitylase treatment and expression was greatly reduced after 4 h of stimulation. These experiments indicated that IRAK1 undergoes degradation after stimulation with R848 for more than 2 h.

Like IRAK1, IRAK2 also became extensively modified by phosphorylation and ubiquitylation in response to R848 (Fig 2D), which was similar in BMDMs from WT mice or IRAK2[E525A] knock-in mice (Fig 2E). The broad “smear” of slowly migrating species was abolished by deubiquitylase treatment, while the most prominent slowly migrating form of IRAK2 was reconverted to the unmodified form by phosphatase treatment (Fig 2F). IRAK2 was fully reconverted to the unmodified form at all time points by treatment with deubiquitylase plus phosphatase. The expression of IRAK2 did not decrease, but started to increase after 3-4 h (Fig 2D). IRAK1 and IRAK2 may therefore function redundantly in the activation of TRAF6 initially, the IRAK2-TRAF6 activation only becoming critical for the activation of the canonical IKK complex when IRAK1 is degraded and/or inactivated.

Decreased production of *il6* and *tnfa* mRNA via the MyD88 signaling pathway after prolonged TLR stimulation in BMDMs from IRAK2[E525A] mice

To investigate the consequence of the loss of IKK activation after prolonged stimulation, we followed the time course of production of the mRNA encoding *il6* and *tnfa*. The production of these mRNAs was similar in BMDMs from IRAK2[E525A] mice and WT mice for up to two hours after stimulation with R848 and partially reduced after stimulation with Pam_3CSK_4 (Figs 3A and 3B). However, the further 100-fold to 1000-fold increase in *il6* mRNA and more modest increase in *tnfa* mRNA observed between 3 and 8 h after stimulation of WT BMDMs was greatly reduced in BMDMs from IRAK2[E525A] mice (Figs 3A and 3B, note that the ordinate for *il6* mRNA production is plotted on a log scale). Consequently, there was virtually no secretion of IL-6 or TNF-α into the cell culture medium after stimulation with R848 or Pam_3CSK_4, or with the TLR9 agonist ODN1826 (hereafter called CpG-B) or the TLR2,6 agonist LTA (Fig 3C). The secretion of MIP1α and MIP1β (Fig 3C), as well as IL-12p40 (results not shown) was also virtually abolished.

To investigate whether the loss of IKKβ activation after prolonged stimulation of BMDM from IRAK2[E525A] knock-in mice could accounts for these results, we added BI605906, an exquisitely specific inhibitor of IKKβ (31), to the cell culture medium 2 h after stimulation with R848 and then monitored subsequent production of *il6* and *tnfa* mRNA over the next few hours. These experiments demonstrated that BI605906 suppressed the R848-stimulated production of *il6* and *tnfa* mRNA (Fig 4A) and the secretion of these cytokines (Fig 4B) in BMDMs from WT mice, similar to the observations made in BMDMs from the IRAK2[E525A] mice in the absence of BI605906 (Fig 3C). Thus the failure to

sustain the activation of IKKβ in BMDMs from the IRAK2[E525A] mice can explain why significant amounts of IL-6 and TNF-α were not produced.

To investigate whether the IRAK2-TRAF6 interaction was required to stimulate gene transcription or enhance mRNA stability, we added actinomycin D to the cell culture medium 90 min after stimulation with R848 and studied the subsequent rate of decay of *il6* and *tnfa* mRNA. We found that the rate at which these pro-inflammatory cytokine mRNAs declined was similar in BMDMs from IRAK2[E525A] and WT mice (Fig 4C), suggesting that the major effect of the loss of the IRAK2-TRAF6 interaction was to suppress gene transcription.

Effect of IRAK2 on the production of some anti-inflammatory molecules

The MyD88 signaling network not only induces the production of pro-inflammatory cytokines but also molecules that restrict the MyD88 signaling network to prevent the overproduction of inflammatory mediators, such as A20 and Dual Specificity Phosphatase 1 (DUSP1), and anti-inflammatory cytokines, such as IL-10. A20 and DUSP1 are immediate early genes that are synthesized within an hour of activating the MyD88-signalling network. A20 is the product of the *tnfaip3* gene, which is dependent on NF-κB (41) and its synthesis therefore requires the activation of the canonical IKK complex, while the induction of DUSP1 is dependent on the activation of mitogen and stress activated protein kinases 1 and 2 (MSK1/MSK2), which are themselves activated by p38α MAPK and ERK1/ERK2 (32, 42).

The R848-stimulated induction of the *tnfaip3* mRNA in BMDMs was maximal after an hour, and was similar in BMDMs from WT mice and IRAK2[E525A] mice (Fig 5A, right hand panel). The level of *tnfaip3* mRNA then declined to half the maximal level, which was sustained from 2 and 8 h in WT BMDMs. In contrast, the level of *tnfaip3* mRNA declined drastically over this period in BMDMs from IRAK2[E525A] mice (Fig 5A, right hand panel), consistent with the essential role of the IRAK2-TRAF6 interaction in sustaining IKKβ activity during prolonged activation of the MyD88 signaling network. The R848-stimulated induction of *dusp1* mRNA in BMDMs also peaked after an hour and was similar in BMDMs from WT or IRAK2[E525A] mice (Fig 5A, left hand panel). This is consistent with similar activation of p38α MAPK and ERK1/ERK2 in BMDMs from the WT and mutant mice during the first hour of R848 stimulation. The *dusp1* mRNA levels declined rapidly after 1 h and the decline was even more marked in BMDMs from the IRAK2[E525A] mice than WT mice (Fig 5A, left hand panel), consistent with reduced MAPK activation after prolonged stimulation with R848 (Fig 2A).

MSK1/MSK2 are not only required for the transcription of the gene encoding DUSP1, but are also important for the transcription of the gene encoding IL-10. MSK1/MSK2 stimulate transcription of the *il10* gene by phosphorylating and activating the transcription factor CREB (32, 42), explaining why, similar to *dusp1* mRNA, the R848 or Pam_3CSK_4-stimulated production of *il10* mRNA peaked after 1 h and then declined over the next few hours (Fig 5B). However, the level of *il10* mRNA increased again from 6 h onwards, which may reflect the time at which CRTC3, a key co-activator of CREB in BMDMs, undergoes dephosphorylation and activation due to inactivation of the protein kinase SIK2 by autocrine factors, such as PGE_2 (43). We found that the early phase of *il10* mRNA production was partially reduced in BMDMs from IRAK2[E525A] mice, but the late phase from 6-8 h was not and was even enhanced in Pam_3CSK4-stimulated macrophages (Fig 5B). Taken together, these findings can explain why the IL-10 secreted into the culture medium was only reduced modestly in BMDMs from IRAK2[E525A] mice when measured after prolonged stimulation with TLR agonists (Fig 5C).

The TRIF signaling pathway is used instead of IRAK2 to sustain the late phase of *il6* and *tnfa* mRNA production by the TLR4 agonist LPS

The LPS-stimulated activation of IKKβ, and MAPKs (Fig 6A) was similar at all time points in BMDMs from IRAK2[E525A] mice and WT mice. Moreover the late, as well as the early, phase of LPS-stimulated *il6*, *tnfa* and *il10* mRNA production (Fig 6B) and the secretion of these molecules (Fig 3C) was only reduced modestly in BMDMs from IRAK2[E525A] mice.

In contrast to other TLRs, which signal solely via MyD88, TLR4 signals via TRIF as well as MyD88, and signaling via both adaptors is required for significant amounts of pro-inflammatory cytokines to be secreted into the culture medium (2, 44). We therefore investigated whether the requirement for the IRAK2-TRAF6 interaction was being replaced by the TRIF signaling pathway in LPS-stimulated macrophages. We found that the activation of IKKβ (as judged by p105 phosphorylation) and MAPKs (Figs 6C), as well as pro-inflammatory cytokine mRNA production up to 2 h (Fig 6D), was similar in BMDMs from $TRIF^{-/-}$ and WT mice. In contrast, the late phase of pro-inflammatory cytokine mRNA production (Fig 6D), and hence cytokine secretion (Fig 6E), was drastically reduced in BMDMs from the $TRIF^{-/-}$ mice. Thus the LPS-stimulated production of pro-inflammatory cytokines in BMDMs from $TRIF^{-/-}$ mice was strikingly similar to the situation seen in BMDMs from IRAK2[E525A] mice after stimulation with R848 or Pam_3CSK_4 (Fig 3).

The LPS-stimulated production of *il10* mRNA in BMDMs from WT and $TRIF^{-/-}$ mice was similar to that observed after stimulation with R848 or Pam_3CSK_4, with a peak at 1 h, followed by a decline up to 4 h and a rise after 6 h (Fig 6D, bottom panel). The decline after 4 h was more marked in BMDMs from $TRIF^{-/-}$ mice similar to the observations made in BMDMs from IRAK2[D525A] mice (Fig 5C). The total amount of IL-10 secreted into the cell culture medium was critically dependent on the times at which this was measured, being decreased after 8 h (Fig 6E) but enhanced after 24 h due to the continued rise in *il10* mRNA between 8 and 24 h (results not shown). This might be explained by the inactivation of SIK2 by autocrine factors (43), as discussed earlier.

IRAK1 catalytic activity is not required for cytokine production in BMDMs

To investigate the role of IRAK1 catalytic activity in the production of inflammatory mediators, we used BMDMs from knock-in mice expressing the catalytically inactive IRAK[D359A] mutant. The R848-stimulated activation of IKKβ and MAPKs (Supplemental Fig. 1B), the production of pro-inflammatory cytokine mRNAs (Supplemental Fig. 1C) and their secretion (Supplemental Fig. 1D) was similar in BMDMs from IRAK1[D359A] mice and WT mice, indicating that IRAK1 catalytic activity was not rate-limiting for IL-6 or TNF-α production under the conditions examined. The LPS-stimulated production of cytokine mRNAs (Supplemental Fig. 1E) and cytokine secretion (Supplemental Fig. 1F), as well as the R848-stimulated secretion of IL-10 (Supplemental Fig. 1D), were little affected in BMDMs from IRAK1[D359A] mice.

IRAK1 catalytic activity as well as IRAK2 function is required for the production of type 1 IFNs by pDCs

Flt3-derived DCs are widely used as a model for studying the function of pDCs and will hereafter be referred to as pDCs. To study the roles of IRAK1 and IRAK2 in IFN production by these cells, we crossed the IRAK2[E525A] mice with the knock-in mice that express the catalytically inactive IRAK1[D359A] mutant and studied IFN production in double knock-in mice as well as the single knock-in mice.

We found that the production of *ifnb*, *ifna4* and *ifna6* mRNA induced by the TLR9 agonist CpG-B (Fig 7A) was virtually abolished in pDCs from the IRAK2[E525A]×IRAK1[D359A] double knock-in mice and, consistent with these findings, the secretion of IFN-α induced by CpG-B, CpG-A and the TLR7 agonist poly(dU) was barely detectable (Fig 8A). In contrast, the CpG-B-stimulated production of *ifnb* mRNA was only reduced slightly in pDCs from the IRAK2[E525A] mice, while the production of *ifna4* was partially reduced and the production of *ifna6* mRNA severely reduced (Fig 7B). Consistent with these findings, there was a partial reduction in the CpG-B, CpG-A and poly(dU) stimulated secretion of IFN-α (Fig 8B). In pDCs from the IRAK1[D359A] mice the CpG-B-stimulated production of *ifnb*, *ifna4* and *ifna6* mRNA was greatly delayed (Fig 7C) and IFN-α secretion measured after 12 hours was reduced (Fig 8C).

IRAK1 and IRAK2 are required to activate IKKβin pDCs

We have reported previously that IKKβ activity plays an essential role in the production of IFN-β in the human pDC cell line Gen2.2 as well as in Flt3-derived dendritic cells, and that IFN-β, as well as IKKβ activity, are required for the production of IFN-α by these cells, as judged by both siRNA "knock-down" experiments and by studies with the specific IKKβ inhibitor BI605906 (23). We therefore investigated the activation of IKKβ in pDCs from IRAK1[D359A], IRAK2[E525A] and the IRAK1[D359A] × IRAK2[E525A] double knock-in mice by monitoring IKKβ phosphorylation at Ser^{177} and Ser^{181}, the amino acid residues whose phosphorylation is required for activation. We found that the activation of IKKβ for the first 3 h after stimulation with CpG-B was unaffected in pDCs from IRAK2[E525A] mice (Fig 8D), delayed considerably in pDCs from IRAK1[D359A] mice (Fig 8E) and abolished in pDCs from IRAK2[E525A] × IRAK1[D359A] mice (Fig 8F), correlating with the observed effects on IFN-β secretion.

The first traces of IFN-β secreted activate the type 1 IFNR, stimulating the activation of members of the Janus family of protein kinases (JAKs), which then phosphorylate and activate STAT1 and STAT2, enabling these transcription factors to stimulate the transcription of IFN-stimulated genes, including the different species of IFN-α. We found that the CpG-B-stimulated phosphorylation of STAT1 at Tyr^{701} was delayed in pDCs from IRAK1[D359A] mice (Fig 8D), reduced in IRAK2[E525A] mice (Fig 8E) and abolished in IRAK1[D359A] × IRAK2[E525A] (Fig 8F), consistent with our previous report that IKKβ activation is required for the production of IFN-β in pDCs and that IKKβ and IFN-β are both required for the production of IFN-α (Fig 9).

We also observed that the expression of STAT1 was reduced significantly in pDCs from the IRAK1[D359A] and IRAK2[E525A] knock-in mice (Figs 8D-8F). This may contribute to the reduced production of phospho-STAT1 and type 1 IFNs, but cannot entirely explain this finding because STAT1 phosphorylation at Tyr^{701} and type I IFN production was abolished in pDCs from the IRAK1[D359A] × IRAK2[E525A] double knock-in mice, even though the expression of STAT1 was not reduced any further than in pDCs from the single knock-in mice..

Discussion

In the present study we generated knock-in mice that express the IRAK2[E525A] mutant that is unable to interact with TRAF6 (Figs 1C-1E) and investigated how the MyD88 signaling network was affected in BMDMs from these animals. The results allowed the MyD88 signaling network to be divided into two phases, an initial phase lasting 1-2 h during which the IRAK2-TRAF6 interaction was not rate limiting, and which was characterized by strong, but transient, activation of the canonical IKK complex and MAPKs; and a second phase from 2-8 hours during which the IRAK2-TRAF6 interaction plays a critical role in

sustaining a low level of activation of the IKK complex (Fig 9A). Although the production of mRNAs encoding pro-inflammatory cytokines, such as IL-6 and TNF-α is initiated during the first 1-2 hours after stimulation, a key role for the initial phase is to rapidly recruit or induce molecules such as A20, ABIN1, DUSP1 and IL-10, that restrict the activation of the MyD88 signaling network. A20 (45-47) and its binding partner ABIN1 (48) dampen the MyD88 signaling network by binding to Lys^{63}-linked and linear polyubiquitin chains that are also formed during the initial phase, while DUSP1 restricts the activation of p38 MAPKs. The failure to produce A20 (49) or inability of ABIN1 to interact with polyubiquitin chains (48), leads to the hyper-activation of the MyD88 signaling network and the overproduction of pro-inflammatory cytokines and leads to autoimmunity. Some of the anti-inflammatory effects of glucocorticoids are blunted in $DUSP1^{-/-}$ mice, highlighting the important role played by DUSP1 in preventing the hyper-activation of p38 MAPKs (50). In summary, a major role of the first phase is to produce molecules needed to ensure that the production of pro-inflammatory cytokines during the second phase is not excessive.

The IRAK2-TRAF6 interaction only became rate limiting for *il6* and *tnfa* mRNA production during the second phase, because IRAK1 was largely degraded 2-4 hours after the activation of the MyD88 signaling network was initiated (Fig 2C). This suggests that the IRAK2 interaction is not rate limiting during the first phase because it operates redundantly with IRAK1 in the activation of TRAF6 during this period. We showed that the IRAK2-TRAF6 interaction was critical during the second phase to sustain a low level of IKKβ (Figs 2A and 2B) without which the surge in *il6* mRNA levels failed to occur and *tnfa* mRNA levels could not be sustained (Figs 3A and 3B). These results explain why the secretion of IL-6, TNF-α and other pro-inflammatory cytokines was virtually abolished in BMDMs from the IRAK2[E525A] mice (Figs 3A-3C). The activation of JNKs, p38 MAPKs and ERK1/2 during the second phase was also reduced in BMDMs from IRAK2[E525A] mice (Fig 2A and 2B) and the IRAK2-TRAF6 interaction is likely to have additional roles during the second phase that have yet to be identified. Importantly, loss of the IRAK2-TRAF6 interaction had relatively little effect on the production the anti-inflammatory molecule DUSP1, which was produced during the first phase when the IRAK2-TRAF6 interaction was not rate limiting. The time course of IL-10 production was complex, but the total amount of IL-10 secreted into the cell culture medium after prolonged activation of the MyD88 signaling network was only reduced modestly in BMDMs from the IRAK2[E525A] mice. The finding the IL-6 and TNF-α secretion was virtually abolished, while overall IL-10 secretion was much less affected in BMDMs from the IRAK2[E525A] mice raises the possibility that IRAK2 could be an interesting target for the development of an anti-inflammatory drug.

A striking finding made during the present study was that the LPS-stimulated production of *il6* and *tnfa* mRNA (Fig 6B) and the secretion of these cytokines (Fig 3C) were only reduced modestly in BMDMs from IRAK2[E525A] mice. LPS activates TLR4, which is unique in signaling via TRIF, as well as via MyD88. The TRIF-dependent signalling pathway does not appear to require members of the IRAK family (14, 51), but instead signals via RIP1 (52), explaining why the LPS-stimulated production of *il6* and *tnfa* mRNA (Fig 6B) was little affected in BMDMs from IRAK2[E525A] mice. However, interestingly, the second but not the first phase of *il6* and *tnfa* mRNA production induced by LPS was greatly reduced in BMDMs from $TRIF^{-/-}$ mice (Fig 6D) mimicking the situation seen when BMDMs from the IRAK2[E525A] mice were stimulated with TLR agonists that only signal via MyD88 (Figs 3A-3C). Taken together, our findings suggest that the TRIF-dependent signalling network is used instead of IRAK2-TRAF6 to sustain the LPS-stimulated *il6* and *tnfa* mRNA production during the second phase (Fig 9B). IRAK2 and the TRIF-dependent pathway clearly do not function redundantly during this stage, otherwise IRAK2 should have been able to compensate for the loss of TRIF in BMDMs from $TRIF^{-/-}$ mice, which was not the case.

The translocation of TLR4 to the endosomes after prolonged stimulation with LPS, from where it can only signal via TRIF (3), may account for these findings.

Our observations with BMDMs from IRAK2[E525A] knock-in mice have revealed similarities and differences to those described previously for macrophages from IRAK2 knockout mice (14, 16). Like macrophages from IRAK2[E525A] mice, macrophages from IRAK2 knockout mice displayed a similar initial activation of NF-κB and MAPKs to WT mice and the secretion of IL-6 and TNF-α was greatly reduced after stimulation with agonists that activate TLRs that signal via MyD88. However, in contrast to the present study, macrophages from the IRAK2 knockout mice showed markedly reduced *il6* and *tnfa* mRNA production after stimulation for 1-2 h with the TLR2 agonist MALP2 (14) and far less IL-6 and TNF-α was secreted in response to LPS (14, 16). IRAK2-deficient mice lack every functional domain of IRAK2, whereas the IRAK2[E525A] mutant only lacks the ability to interact with TRAF6. Therefore, the loss of the other functional domains of IRAK2 may account for these differences.

We were unable to detect any significant impairment in the activation of the canonical IKK complex and MAPKs, the production of *il6* and *tnfa* mRNA or their secretion in BMDMs from mice expressing the catalytically inactive IRAK1[D359A] mutant. These results are consistent with earlier studies from other laboratories in which the overexpression of a catalytically inactive mutant of IRAK1 was shown to stimulate NF-κB-dependent gene transcription similarly to WT IRAK1 (53) and to restore the IL-1-stimulated signaling network in IRAK1-null IL-1R cells (39). However, in contrast with BMDMs, we found that the catalytic activity of IRAK1 was critical for the production of type 1 IFNs in pDCs, which led us to study the relative roles of IRAK1 and IRAK2 in IFN production by TLR9 and TLR7 agonists. The production of IFNs in pDCs can also be divided into two phases, an initial phase lasting 3-4 h during which the production and secretion of IFN-β is initiated. IFN-β then activates the JAK-STAT signaling network by an autocrine mechanism, initiating a positive feedback loop that further enhances the production of IFN-β and triggers the production of IFN-α during the second phase (54, 55) (Fig 9C). We found that IRAK1 catalytic activity plays a key role in IFN-β production during the first phase and hence is also important for the production of IFN-α during the second phase (Figs 7C and 8C). In contrast, the IRAK2-TRAF6 interaction was not rate-limiting for the production of IFN-β but made an important contribution to the production of IFN-α during the second phase (Figs 7B and 8B). The production of IFN-α and IFN-β was abolished in pDCs from mice lacking both a catalytically inactive IRAK1 and a functionally inactive IRAK2 (Figs 7A and 8A).

We have reported previously that IKKβ activity is essential for *ifnb* mRNA production in response to TLR7 and TLR9 agonists in both mouse pDCs and the human Gen2.2 pDC cell line (23) and that IFN-β and IKKβ were both required for the subsequent production of IFN-α. In the present study, we again found a striking correlation between the degree of activation of IKKβ and the production of *ifnβ* mRNA in CpG B-stimulated pDCs. Thus the activation of IKKβ and *ifnb* mRNA production were delayed in pDCs from IRAK1[D359A] mice, little unaffected in IRAK2[E525A] mice and abolished in pDCs from IRAK2[E525A] × IRAK1[D359A] mice (Figs 7 and 8). The molecular mechanism by which IKKβ stimulates IFN production has yet to be defined, but is at least partially independent of NF-κB (23, 24). In summary, a key role for the catalytic activity of IRAK1 and the IRAK2-TRAF6 interaction in pDCs is to activate IKKβ, although other essential roles for these IRAKs in IFN production is not excluded. For example, IKKα is also known to play an essential role in IFN production by pDCs (21). In summary, a key role of IRAK2 in both pro-inflammatory cytokine production in BMDMs and type 1 IFN production in pDCs is to

sustain the activation of key signaling components, such as IKKα and IKKβ, after prolonged activation of TLRs that signal via MyD88.

To our knowledge, our study provides the first genetic evidence that the catalytic activity of IRAK1 is critical for *ifn* mRNA production and IFN secretion by pDCs, although a requirement for IRAK1 catalytic activity to produce IFN was suggested previously from the observation that the overexpression of a catalytically inactive mutant of IRAK1 blocked transcription from an IFN-α4 reporter gene induced by the co-transfection of MyD88 and IRF7 into HEK293 cells (25). Since IRAK1 catalytic activity is critical for type 1 interferon production by pDCs, but is not required for cytokine production by macrophages, specific inhibitors of IRAK1 merit evaluation for the treatment of autoimmune diseases that have been linked to the overproduction of type 1 IFNs by pDCs (20).

In contrast to the present study in which we have shown IRAK2 to be a positive regulator of IFN-α production in pDCs, other investigators reported that IFN-α production was enhanced in pDCs from IRAK2 knockout mice after stimulation with a TLR9 agonist or during viral infection, and concluded that IRAK2 was a negative regulator of IFN production (26). In pDCs from IRAK2 knockout mice, IFN production is presumably driven solely by the MyD88-IRAK4-IRAK1 oligomeric complex, which may stimulate IFN production more strongly than the MyD88-IRAK4-IRAK1/2 module, and so enhance IFN production in pDCs from IRAK2 knockout mice. However, our results clearly show that IRAK2 is not a negative regulator but a positive regulator of IFN-α production in WT pDCs. Our findings highlight a potential difficulty in interpreting results obtained by studies on cells from knock-out mice in which every functional domain of a complex multi-domain protein is deleted, and demonstrate the potential power of studying knock-in mice in which just a single functional domain of a protein is disabled to gain a deeper insight into the operation of innate immune signaling networks.

Supplementary Material

Refer to Web version on PubMed Central for supplementary material.

Acknowledgments

We are grateful to Drs Xiaoxia Li and George Stark (Cleveland, OH) for generously providing IL-1R and IRAK1-null IL-1R cells. We also thank the Transgenic Mouse Facility at the University of Dundee for help in generating the IRAK1[D359A] and IRAK2[E525A] knock-in mice, Julia Carr and Gail Fraser for the mouse genotyping and Mark Peggie for cloning mouse IRAK1, IRAK2 and TRAF6.

The work was supported by a Wellcome Trust Senior Investigator Award (to P.C.), the UK Medical Research Council, AstraZeneca, Boehringer-Ingelheim, GlaxoSmithKline, Janssen Pharmaceutica, Merck-Serono and Pfizer.

Abbreviations used in this article

BMDM	bone marrow-derived macrophage
DC	dendritic cell
DD	death domain
DUSP1	Dual Specificity Phosphatase 1
ES	embryonic stem
HEK293	human embryonic kidney 293
IKK	IκB-inducing kinase

IRAK	IL-1R-accociated kinase
LTA	lipoteichoic acid
MALP2	macrophage-activating lipopeptide 2
MSK1/MSK2	mitogen- and stress-activated protein kinases 1 and 2
pDC	plasmacytoid dendritic cell
poly(dU)	poly(deoxyuridylic acid)
TAB	TGFβ-activated kinase 1 binding protein
TAK1	TGFβ-activated kinase 1
TRAF6	TNFRassociated factor 6
TRIF	Toll/IL-1R domain-containing-adapter-inducing IFN-β
USP2	ubiquitin-specific protease 2
WT	wild type

References

1. Hidmark A, von Saint Paul A, Dalpke AH. Cutting edge: TLR13 is a receptor for bacterial RNA. J Immunol. 2012; 189:2717–2721. [PubMed: 22896636]
2. Kawai T, Akira S. The role of pattern-recognition receptors in innate immunity: update on Toll-like receptors. Nat Immunol. 2010; 11:373–384. [PubMed: 20404851]
3. Kagan JC, Su T, Horng T, Chow A, Akira S, Medzhitov R. TRAM couples endocytosis of Toll-like receptor 4 to the induction of interferon-beta. Nat Immunol. 2008; 9:361–368. [PubMed: 18297073]
4. Lin SC, Lo YC, Wu H. Helical assembly in the MyD88-IRAK4-IRAK2 complex in TLR/IL-1R signalling. Nature. 2010; 465:885–890. [PubMed: 20485341]
5. Motshwene PG, Moncrieffe MC, Grossmann JG, Kao C, Ayaluru M, Sandercock AM, Robinson CV, Latz E, Gay NJ. An oligomeric signaling platform formed by the Toll-like receptor signal transducers MyD88 and IRAK-4. J Biol Chem. 2009; 284:25404–25411. [PubMed: 19592493]
6. Ye H, Arron JR, Lamothe B, Cirilli M, Kobayashi T, Shevde NK, Segal D, Dzivenu OK, Vologodskaia M, Yim M, Du K, Singh S, Pike JW, Darnay BG, Choi Y, Wu H. Distinct molecular mechanism for initiating TRAF6 signalling. Nature. 2002; 418:443–447. [PubMed: 12140561]
7. Wang C, Deng L, Hong M, Akkaraju GR, Inoue J, Chen ZJ. TAK1 is a ubiquitin-dependent kinase of MKK and IKK. Nature. 2001; 412:346–351. [PubMed: 11460167]
8. Xia ZP, Sun L, Chen X, Pineda G, Jiang X, Adhikari A, Zeng W, Chen ZJ. Direct activation of protein kinases by unanchored polyubiquitin chains. Nature. 2009; 461:114–119. [PubMed: 19675569]
9. Rahighi S, Ikeda F, Kawasaki M, Akutsu M, Suzuki N, Kato R, Kensche T, Uejima T, Bloor S, Komander D, Randow F, Wakatsuki S, Dikic I. Specific recognition of linear ubiquitin chains by NEMO is important for NF-kappaB activation. Cell. 2009; 136:1098–1109. [PubMed: 19303852]
10. Tokunaga F, Sakata S, Saeki Y, Satomi Y, Kirisako T, Kamei K, Nakagawa T, Kato M, Murata S, Yamaoka S, Yamamoto M, Akira S, Takao T, Tanaka K, Iwai K. Involvement of linear polyubiquitylation of NEMO in NF-kappaB activation. Nat Cell Biol. 2009; 11:123–132. [PubMed: 19136968]
11. Waterfield M, Jin W, Reiley W, Zhang M, Sun SC. IkappaB kinase is an essential component of the Tpl2 signaling pathway. Mol Cell Biol. 2004; 24:6040–6048. [PubMed: 15199157]
12. Lang V, Symons A, Watton SJ, Janzen J, Soneji Y, Beinke S, Howell S, Ley SC. ABIN-2 forms a ternary complex with TPL-2 and NF-kappa B1 p105 and is essential for TPL-2 protein stability. Mol Cell Biol. 2004; 24:5235–5248. [PubMed: 15169888]

13. Dumitru CD, Ceci JD, Tsatsanis C, Kontoyiannis D, Stamatakis K, Lin JH, Patriotis C, Jenkins NA, Copeland NG, Kollias G, Tsichlis PN. TNF-alpha induction by LPS is regulated posttranscriptionally via a Tpl2/ERK-dependent pathway. Cell. 2000; 103:1071–1083. [PubMed: 11163183]
14. Kawagoe T, Sato S, Matsushita K, Kato H, Matsui K, Kumagai Y, Saitoh T, Kawai T, Takeuchi O, Akira S. Sequential control of Toll-like receptor-dependent responses by IRAK1 and IRAK2. Nat Immunol. 2008; 9:684–691. [PubMed: 18438411]
15. Swantek JL, Tsen MF, Cobb MH, Thomas JA. IL-1 receptor-associated kinase modulates host responsiveness to endotoxin. J Immunol. 2000; 164:4301–4306. [PubMed: 10754329]
16. Wan Y, Xiao H, Affolter J, Kim TW, Bulek K, Chaudhuri S, Carlson D, Hamilton T, Mazumder B, Stark GR, Thomas J, Li X. Interleukin-1 receptor-associated kinase 2 is critical for lipopolysaccharide-mediated post-transcriptional control. J Biol Chem. 2009; 284:10367–10375. [PubMed: 19224918]
17. Gilliet M, Cao W, Liu YJ. Plasmacytoid dendritic cells: sensing nucleic acids in viral infection and autoimmune diseases. Nat Rev Immunol. 2008; 8:594–606. [PubMed: 18641647]
18. Trinchieri G. Type I interferon: friend or foe? J Exp Med. 2010; 207:2053–2063. [PubMed: 20837696]
19. Barrat FJ, Meeker T, Gregorio J, Chan JH, Uematsu S, Akira S, Chang B, Duramad O, Coffman RL. Nucleic acids of mammalian origin can act as endogenous ligands for Toll-like receptors and may promote systemic lupus erythematosus. J Exp Med. 2005; 202:1131–1139. [PubMed: 16230478]
20. Banchereau J, Pascual V. Type I interferon in systemic lupus erythematosus and other autoimmune diseases. Immunity. 2006; 25:383–392. [PubMed: 16979570]
21. Hoshino K, Sugiyama T, Matsumoto M, Tanaka T, Saito M, Hemmi H, Ohara O, Akira S, Kaisho T. IkappaB kinase-alpha is critical for interferon-alpha production induced by Toll-like receptors 7 and 9. Nature. 2006; 440:949–953. [PubMed: 16612387]
22. Hoshino K, Sasaki I, Sugiyama T, Yano T, Yamazaki C, Yasui T, Kikutani H, Kaisho T. Critical role of IkappaB Kinase alpha in TLR7/9-induced type I IFN production by conventional dendritic cells. J Immunol. 2010; 184:3341–3345. [PubMed: 20200270]
23. Pauls E, Shpiro N, Peggie M, Young EM, Sorcek RT, Tan L, Choi HG, Cohen P. An essential role for IKKbeta in the production of type 1 interferons by plasmacytoid dendritic cells. J Biol Chem. 2012; 287:19216–19228. [PubMed: 22511786]
24. Wang X, Hussain S, Wang EJ, Li MO, Garcia-Sastre A, Beg AA. Lack of essential role of NF-kappa B p50, RelA, and cRel subunits in virus-induced type 1 IFN expression. J Immunol. 2007; 178:6770–6776. [PubMed: 17513724]
25. Uematsu S, Sato S, Yamamoto M, Hirotani T, Kato H, Takeshita F, Matsuda M, Coban C, Ishii KJ, Kawai T, Takeuchi O, Akira S. Interleukin-1 receptor-associated kinase-1 plays an essential role for Toll-like receptor (TLR)7- and TLR9-mediated interferon-{alpha} induction. J Exp Med. 2005; 201:915–923. [PubMed: 15767370]
26. Wan Y, Kim TW, Yu M, Zhou H, Yamashita M, Kang Z, Yin W, Wang JA, Thomas J, Sen GC, Stark GR, Li X. The dual functions of IL-1 receptor-associated kinase 2 in TLR9-mediated IFN and proinflammatory cytokine production. Journal of immunology. 2011; 186:3006–3014.
27. Flannery S, Bowie AG. The interleukin-1 receptor-associated kinases: critical regulators of innate immune signalling. Biochem Pharmacol. 2010; 80:1981–1991. [PubMed: 20599782]
28. Wesche H, Gao X, Li X, Kirschning CJ, Stark GR, Cao Z. IRAK-M is a novel member of the Pelle/interleukin-1 receptor-associated kinase (IRAK) family. J Biol Chem. 1999; 274:19403–19410. [PubMed: 10383454]
29. Hardy MP, O'Neill LA. The murine IRAK2 gene encodes four alternatively spliced isoforms, two of which are inhibitory. J Biol Chem. 2004; 279:27699–27708. [PubMed: 15082713]
30. Conner JR, Smirnova, Poltorak A. A mutation in Irak2c identifies IRAK-2 as a central component of the TLR regulatory network of wild-derived mice. J Exp Med. 2009; 206:1615–1631. [PubMed: 19564352]

31. Clark K, Peggie M, Plater L, Sorcek RJ, Young ER, Madwed JB, Hough J, McIver EG, Cohen P. Novel cross-talk within the IKK family controls innate immunity. Biochem J. 2011; 434:93–104. [PubMed: 21138416]
32. Wiggin GR, Soloaga A, Foster JM, Murray-Tait V, Cohen P, Arthur JS. MSK1 and MSK2 are required for the mitogen- and stress-induced phosphorylation of CREB and ATF1 in fibroblasts. Mol Cell Biol. 2002; 22:2871–2881. [PubMed: 11909979]
33. Knighton DR, Zheng JH, Ten Eyck LF, Ashford VA, Xuong NH, Taylor SS, Sowadski JM. Crystal structure of the catalytic subunit of cyclic adenosine monophosphate-dependent protein kinase. Science. 1991; 253:407–414. [PubMed: 1862342]
34. Goh ET, Arthur JS, Cheung PC, Akira S, Toth R, Cohen P. Identification of the protein kinases that activate the E3 ubiquitin ligase Pellino 1 in the innate immune system. Biochem J. 2012; 441:339–346. [PubMed: 22007846]
35. Naik SH, O'Keeffe M, Proietto A, Shortman HH, Wu L. CD8+, CD8−, and plasmacytoid dendritic cell generation in vitro using flt3 ligand. Methods Mol Biol. 2010; 595:167–176. [PubMed: 19941111]
36. Windheim M, Stafford M, Peggie M, Cohen P. Interleukin-1 (IL-1) induces the Lys63-linked polyubiquitination of IL-1 receptor-associated kinase 1 to facilitate NEMO binding and the activation of IkappaBalpha kinase. Mol Cell Biol. 2008; 28:1783–1791. [PubMed: 18180283]
37. Clark K, Mackenzie KF, Petkevicius K, Kristariyanto Y, Zhang J, Choi HG, Peggie M, Plater L, Pedrioli PG, McIver E, Gray NS, Arthur JS, Cohen P. Phosphorylation of CRTC3 by the salt-inducible kinases controls the interconversion of classically activated and regulatory macrophages. Proc Natl Acad Sci U S A. 2012; 109:16986–16991. [PubMed: 23033494]
38. Keating SE, Maloney GM, Moran EM, Bowie AG. IRAK-2 participates in multiple toll-like receptor signaling pathways to NFkappaB via activation of TRAF6 ubiquitination. J Biol Chem. 2007; 282:33435–33443. [PubMed: 17878161]
39. Li X, Commane M, Burns C, Vithalani K, Cao Z, Stark GR. Mutant cells that do not respond to interleukin-1 (IL-1) reveal a novel role for IL-1 receptor-associated kinase. Mol Cell Biol. 1999; 19:4643–4652. [PubMed: 10373513]
40. Beinke S, Robinson MJ, Hugunin M, Ley SC. Lipopolysaccharide activation of the TPL-2/MEK/extracellular signal-regulated kinase mitogen-activated protein kinase cascade is regulated by IkappaB kinase-induced proteolysis of NF-kappaB1 p105. Mol Cell Biol. 2004; 24:9658–9667. [PubMed: 15485931]
41. Opipari AW Jr. Boguski MS, Dixit VM. The A20 cDNA induced by tumor necrosis factor alpha encodes a novel type of zinc finger protein. The Journal of biological chemistry. 1990; 265:14705–14708. [PubMed: 2118515]
42. Ananieva O, Darragh J, Johansen C, Carr JM, McIlrath J, Park JM, Wingate A, Monk CE, Toth R, Santos SG, Iversen L, Arthur JS. The kinases MSK1 and MSK2 act as negative regulators of Toll-like receptor signaling. Nat Immunol. 2008; 9:1028–1036. [PubMed: 18690222]
43. MacKenzie KF, Clark K, Naqvi S, McGuire VA, Noehren G, Kristariyanto Y, van den Bosch M, Mudaliar M, McCarthy PC, Pattison MJ, Pedrioli PG, Barton GJ, Toth R, Prescott A, Arthur JS. PGE(2) induces macrophage IL-10 production and a regulatory-like phenotype via a protein kinase A-SIK-CRTC3 pathway. Journal of immunology. 2013; 190:565–577.
44. Yamamoto M, Sato S, Hemmi H, Hoshino K, Kaisho T, Sanjo H, Takeuchi O, Sugiyama M, Okabe M, Takeda K, Akira S. Role of adaptor TRIF in the MyD88-independent toll-like receptor signaling pathway. Science. 2003; 301:640–643. [PubMed: 12855817]
45. Verhelst K, Carpentier I, Kreike M, Meloni L, Verstrepen L, Kensche T, Dikic I, Beyaert R. A20 inhibits LUBAC-mediated NF-kappaB activation by binding linear polyubiquitin chains via its zinc finger 7. The EMBO journal. 2012; 31:3845–3855. [PubMed: 23032186]
46. Skaug B, Chen J, Du F, He J, Ma A, Chen ZJ. Direct, noncatalytic mechanism of IKK inhibition by A20. Mol Cell. 2011; 44:559–571. [PubMed: 22099304]
47. Tokunaga F, Nishimasu H, Ishitani R, Goto E, Noguchi T, Mio K, Kamei K, Ma A, Iwai K, Nureki O. Specific recognition of linear polyubiquitin by A20 zinc finger 7 is involved in NF-kappaB regulation. The EMBO journal. 2012; 31:3856–3870. [PubMed: 23032187]

48. Nanda SK, Venigalla RK, Ordureau A, Patterson-Kane JC, Powell DW, Toth R, Arthur JS, Cohen P. Polyubiquitin binding to ABIN1 is required to prevent autoimmunity. The Journal of experimental medicine. 2011; 208:1215–1228. [PubMed: 21606507]

49. Lee EG, Boone DL, Chai S, Libby SL, Chien M, Lodolce JP, Ma A. Failure to regulate TNF-induced NF-kappaB and cell death responses in A20-deficient mice. Science. 2000; 289:2350–2354. [PubMed: 11009421]

50. Abraham SM, Lawrence T, Kleiman A, Warden P, Medghalchi M, Tuckermann J, Saklatvala J, Clark AR. Antiinflammatory effects of dexamethasone are partly dependent on induction of dual specificity phosphatase 1. The Journal of experimental medicine. 2006; 203:1883–1889. [PubMed: 16880258]

51. Kawagoe T, Sato S, Jung A, Yamamoto M, Matsui K, Kato H, Uematsu S, Takeuchi O, Akira S. Essential role of IRAK-4 protein and its kinase activity in Toll-like receptor-mediated immune responses but not in TCR signaling. J Exp Med. 2007; 204:1013–1024. [PubMed: 17485511]

52. Meylan E, Burns K, Hofmann K, Blancheteau V, Martinon F, Kelliher M, Tschopp J. RIP1 is an essential mediator of Toll-like receptor 3-induced NF-kappa B activation. Nature immunology. 2004; 5:503–507. [PubMed: 15064760]

53. Maschera B, Ray K, Burns K, Volpe F. Overexpression of an enzymically inactive interleukin-1-receptor-associated kinase activates nuclear factor-kappaB. Biochem J. 1999; 339(Pt 2):227–231. [PubMed: 10191251]

54. Honda K, Yanai H, Negishi H, Asagiri M, Sato M, Mizutani T, Shimada N, Ohba Y, Takaoka A, Yoshida N, Taniguchi T. IRF-7 is the master regulator of type-I interferon-dependent immune responses. Nature. 2005; 434:772–777. [PubMed: 15800576]

55. Sato M, Suemori H, Hata N, Asagiri M, Ogasawara K, Nakao K, Nakaya T, Katsuki M, Noguchi S, Tanaka N, Taniguchi T. Distinct and essential roles of transcription factors IRF-3 and IRF-7 in response to viruses for IFN-alpha/beta gene induction. Immunity. 2000; 13:539–548. [PubMed: 11070172]

Europe PMC Funders Author Manuscripts

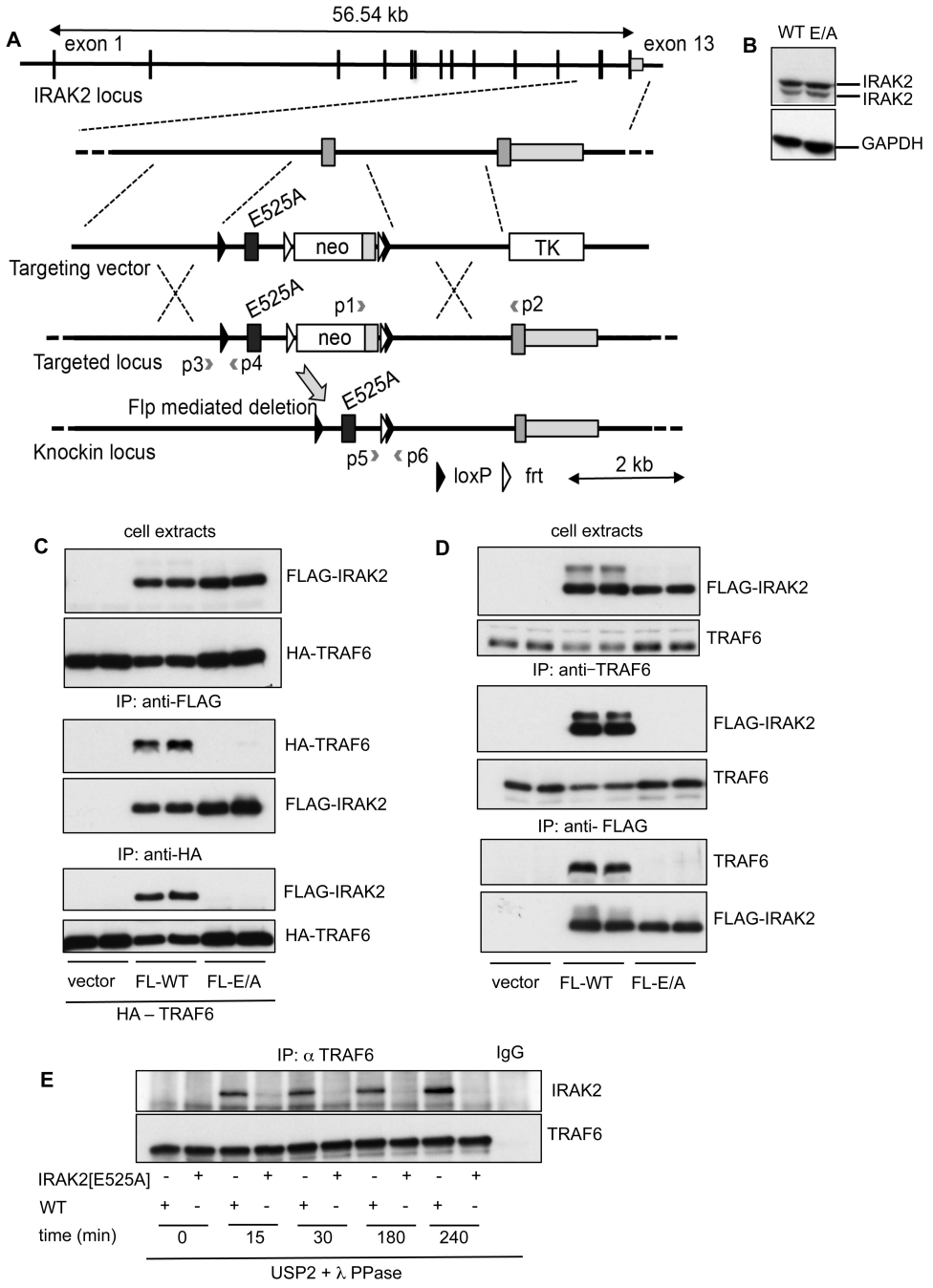

Figure 1. Generation of an IRAK2[E525A] knock-in mice

(**A**) Mice were generated in which Glu^{525} of IRAK2 was mutated to Ala using the strategy detailed in *Materials and Methods*. The polyA-trapping neomycin cassette was used for positive selection, which allowed ES cell colonies to be screened by reverse transcription PCR of mRNA using the primers indicated (p1 and p2). This generated a 317-bp band in correctly targeted clones. The presence of the 5′ loxP site was confirmed by PCR of genomic DNA using primers p2 and p3. Correctly targeted ES cell clones were used to generate chimeric mice, and germline transmitting chimeric mice crossed to mice containing an Flp*e* transgene to excise the neomycin gene. Excision of this gene was confirmed by PCR

using primers p5 and p6. (**B**) BMDM lysates (10 μg protein) from WT or IRAK2[E525A] (E/A) mice were immuno-blotted with the antibodies indicated. (**C**) IRAK1-null IL-1R HEK293 cells were co-transfected with plasmids encoding HA-tagged mouse TRAF6 (HA-TRAF6) or an empty vector (vector), and either FLAG-mouse WT IRAK2 (FL-WT) or FLAG-mouse IRAK2[E525A](FL-E/A). After 24 h, the cells were lysed and cell extracts subjected to SDS-PAGE and immuno-blotting with anti-HA or anti-FLAG to monitor the expression of TRAF6 and IRAK2 (*top two panels*). The FLAG-tagged IRAK2 (*middle two panels*) or HA-tagged TRAF6 (*bottom two panels*) were immunoprecipitated from 0.25 mg of cell extract protein then denatured in SDS subjected to SDS-PAGE and immuno-blotted with either anti-HA or anti-FLAG antibodies. (**D**) The experiment was carried out as in (C), except that HA-TRAF6 was omitted from all transfections. In the *middle two panels* the endogenous human TRAF6 in the cells was immunoprecipitated from 0.5 mg cell extract protein and the presence of FLAG-IRAK2 (FL-WT) or FLAG-IRAK2[E525A] (FL-E/A) in the immunoprecipitates was detected by immunoblotting with anti-FLAG. In the *bottom two panels*, FLAG-IRAK2[WT] (FL-WT) or FLAG-IRAK2[E525A] (FL-E/A) were immunoprecipitated and the presence of the endogenous human TRAF6 was detected by immunoblotting. (**E**) Primary BMDMs were stimulated with 1.0 μg/ml R848 for the times indicated. The cells were lysed and TRAF6 immunoprecipitated from the cell extracts and treated with USP2 and phage λ phosphatase to deubiquitylate and dephosphorylate IRAK2 (see *Materials and Methods*). Proteins were released from the antibody-Sepharose conjugate by denaturation in SDS and the supernatants subjected to SDS-PAGE and immuno-blotting with the antibodies indicated.

Europe PMC Funders Author Manuscripts

Europe PMC Funders Author Manuscripts

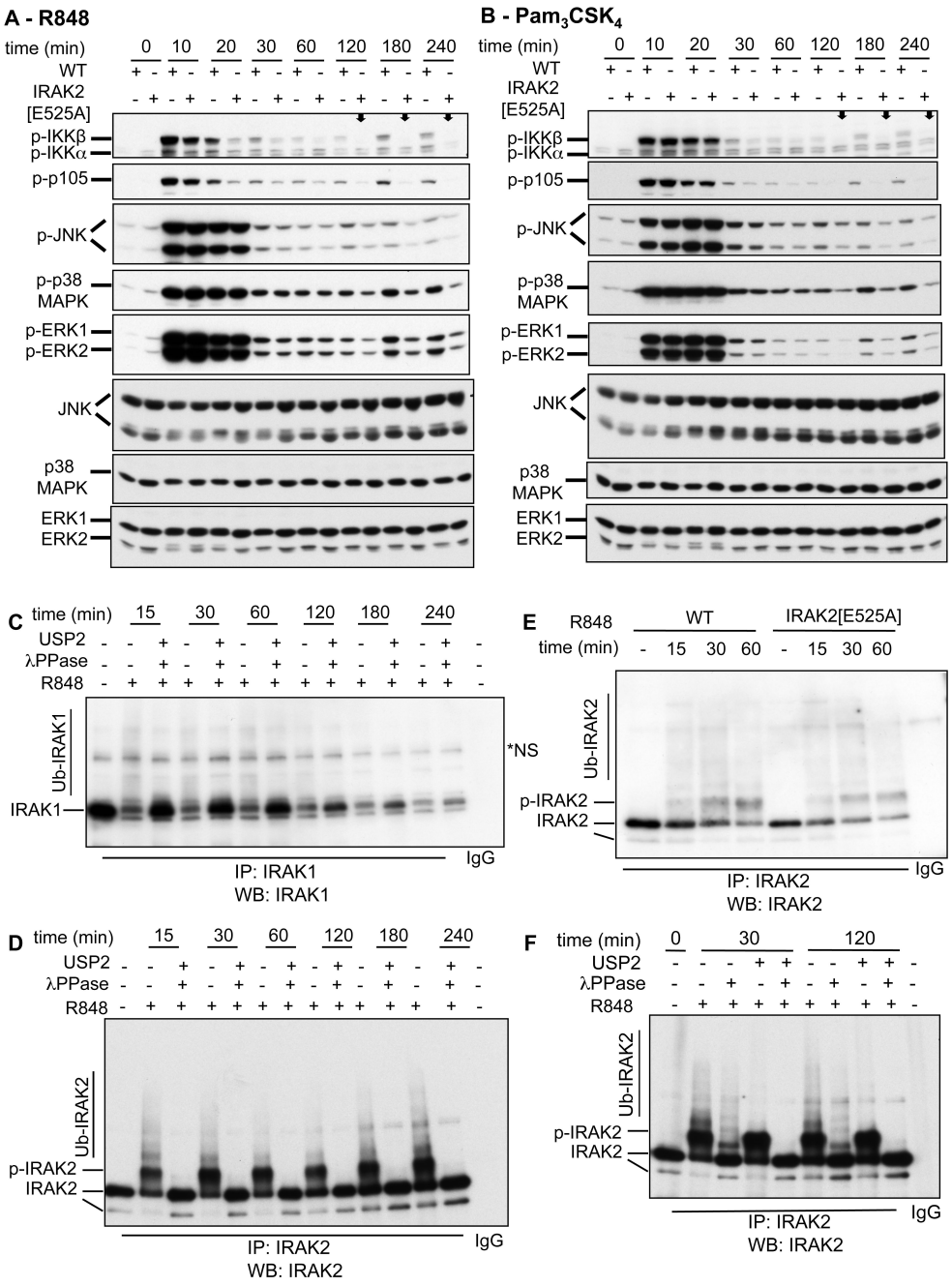

Figure 2. The activation and expression of signaling components of the MyD88 network in BMDM from IRAK2[E525A] mice during prolonged stimulation with TLR agonists

(**A, B**) BMDMs from WT (IRAK2[WT]) and IRAK2[E525A] mice were stimulated for the times indicated with 1 μg/ml R848 (A) or 1 μg/ml Pam_3CSK_4 (B). Cell extract protein (10 μg) was denatured in SDS, subjected to SDS-PAGE and immunoblotted with the indicated antibodies. Similar results were obtained in three separate experiments. **(C, D)** Primary WT BMDMs (prepared using L929 preconditioned medium) were stimulated for the times indicated with 1 μg/ml R848. The cells were lysed and IRAK1 (C) or IRAK2 (D) immunoprecipitated from the cell extracts and treated with (+) or without (−) USP2 and phage λ phosphatase as described in *Materials and Methods*. The reactions were terminated

in SDS and after removal of the protein G-agarose, the supernatants were subjected to SDS-PAGE and immunoblotted with the antibodies indicated. (**E**) As in (D), except that IRAK2 was immunoprecipitated from the extracts of WT or IRAK2[E525A] mice. (**F**) As in (D), except that the IRAK2 immunoprecipitates were incubated with (+) or without (−) USP2 and/or phage λ phosphatase. Data are representative of two to three independent experiments. *NS, non-specific band.

Europe PMC Funders Author Manuscripts

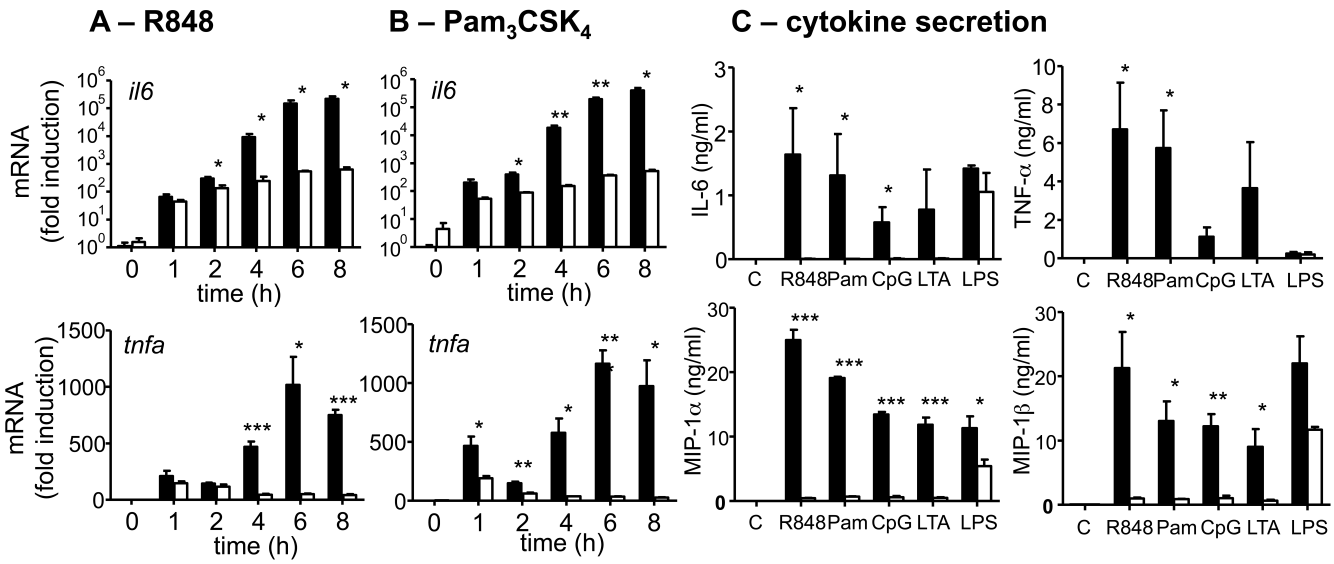

Figure 3. Reduced cytokine production in BMDMs from IRAK2[E525A] mice after prolonged stimulation with TLR agonists

(**A, B**) BMDMs from WT (black bars) and IRAK2[E525A] (white bars) mice were incubated for the times indicated in the presence of 1 μg/ml R848 (**A**) or 1 μg/ml Pam_3CSK_4 (B). RNA was extracted from the cells and *il6* and *tnfa* mRNA was measured by quantitative real-time PCR. The results are plotted as the fold increase in mRNA relative to the level determined in unstimulated cells. Error bars represent the mean ± SEM for experiments with BMDMs from three mice of each genotype. The data shown are representative of three independent experiments. (**C**) BMDMs from WT (black bars) or IRAK2[E525A] (white bars) mice were incubated for 7 h in the absence of any agonist (control [C]), 1 μg/ml R848, 1 μg/ml Pam_3CSK_4 (Pam), 2 μM ODN1826 (CpG), 1 μg/ml LTA, or 100 ng/ml LPS. The concentrations of IL-6, TNF-α, MIP1α and MIP1β in the supernatant were then measured. Error bars represent the mean ± SD for experiments with BMDMs from three mice of each genotype. The data shown are representative of three independent experiments. *$p \leq 0.05$, **$p \leq 0.005$, ***$p \leq 0.0005$.

Europe PMC Funders Author Manuscripts

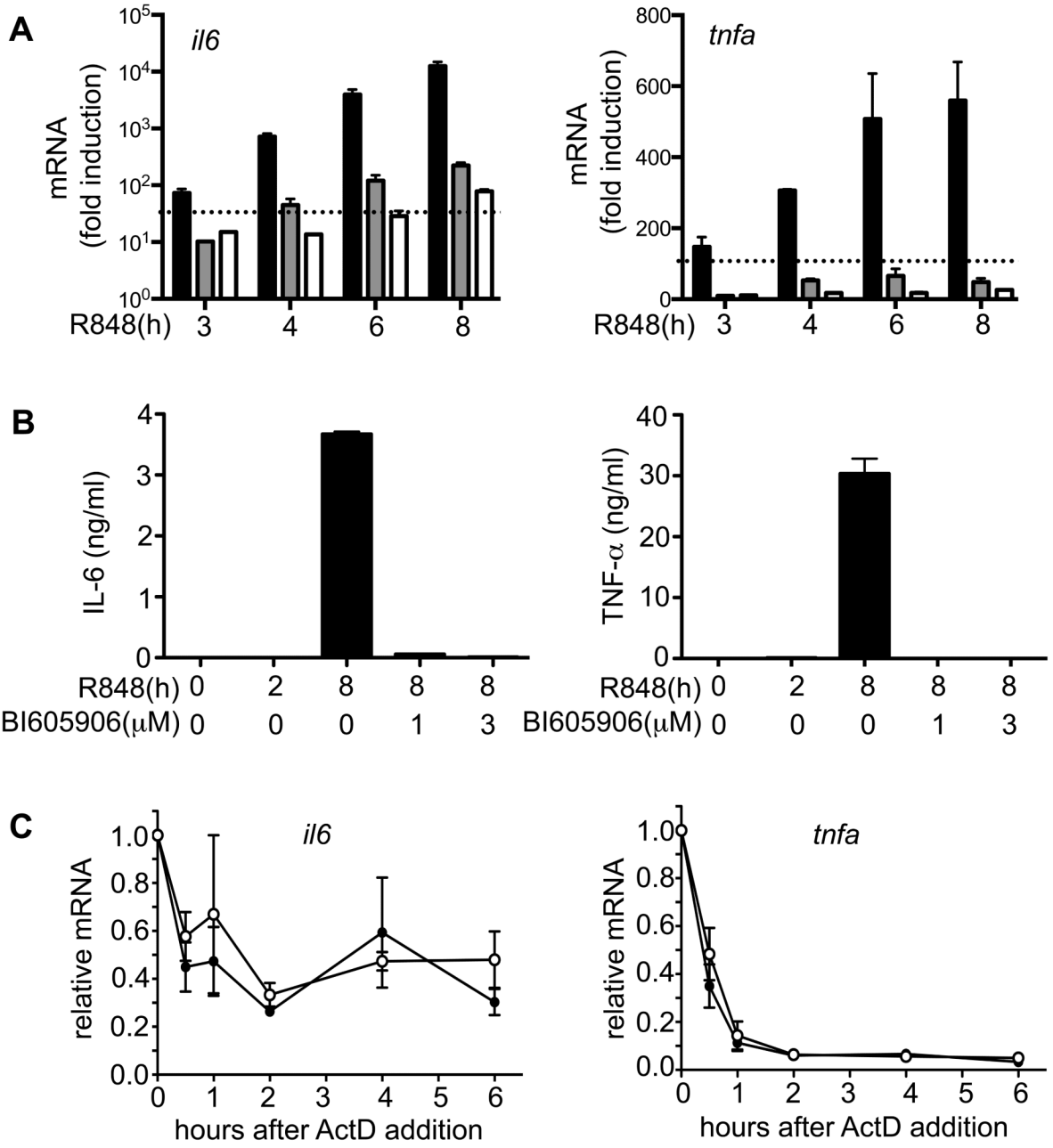

Figure 4. Inhibition of IKKβ leads to suppression of pro-inflammatory cytokine production

(**A**) BMDMs from WT mice were stimulated for 2 h with 1.0 μg/ml R848. The IKKβ inhibitor BI605906 was then added to the culture medium to a concentration of 1.0 μM (grey bars) or 3.0 μM (white bars). The black bars show a control experiment in which no inhibitor was added after 2 h. RNA was extracted from the cells at each time point, and *il6* and *tnfa* mRNA was measured by quantitative real-time PCR. Results are plotted as the fold increase in mRNA relative to the level determined in unstimulated cells, and the broken line indicates the amount of mRNA produced after 2 h before the addition of BI605906. Error bars show the average of duplicate determinations for each condition. Data shown are

representative of two independent experiments. (**B**) Cell culture supernatants from (A) were collected and the concentrations of IL-6 and TNF-α were measured. (**C**) BMDM from either WT (○) or IRAK2[E525A] mice (●) were stimulated for 1.5 h with 1.0 μg/ml R848 and actinomycin D (ActD) was added to the culture medium to a final concentration of 5 μg/ml. Stimulation with R848 was continued and RNA was extracted from the cells at the times indicated and *il6* (*left panel*) and *tnfa* (*right panel*) mRNA was measured by qPCR. The ordinate shows the mRNA levels at each time point relative that measured at the time of ActD addition (1.0). Error bars represent the mean ± SEM for experiments with BMDM from three mice of each genotype. Data shown are representative of two independent experiments.

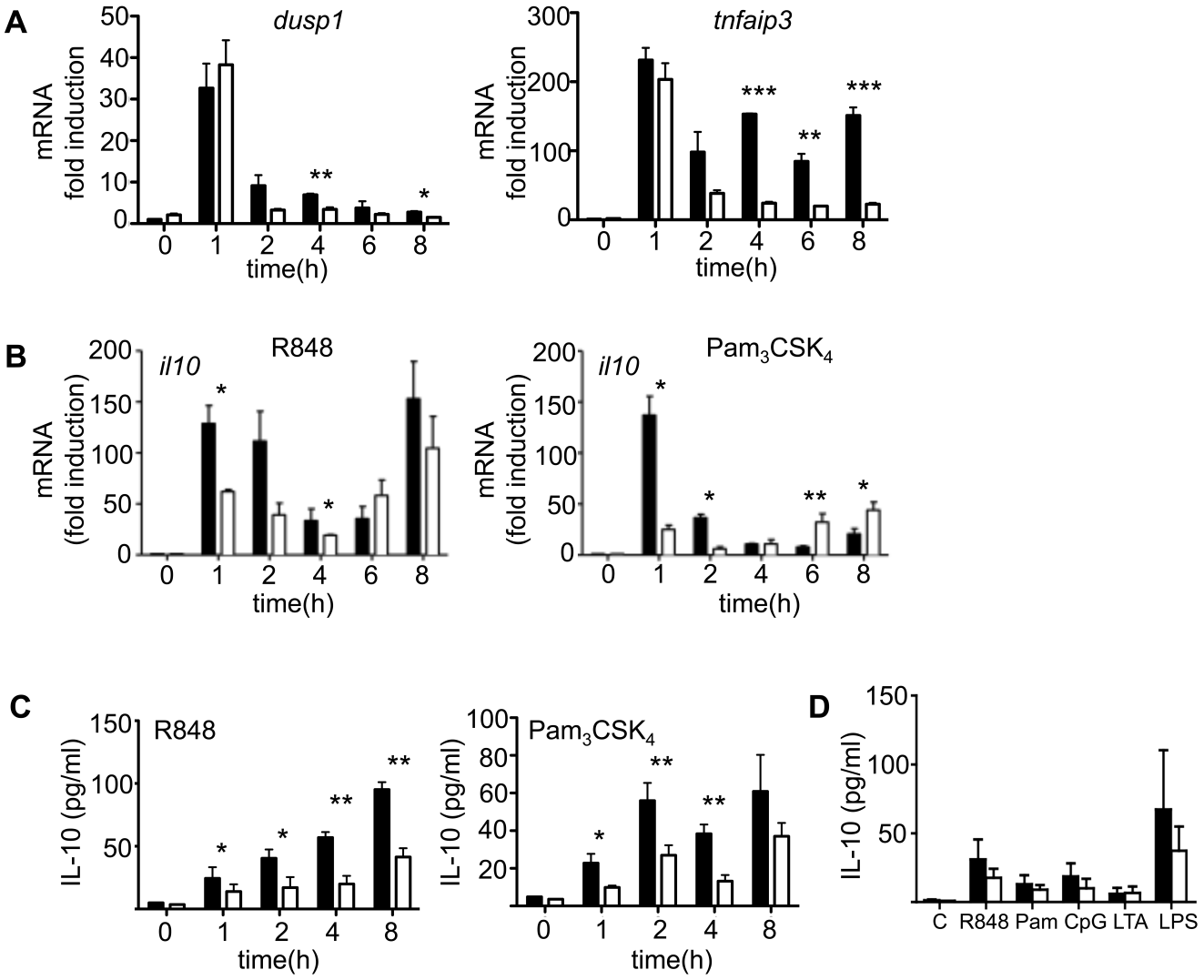

Figure 5. Effect of loss of the IRAK2-TRAF6 interaction on the production of some anti-inflammatory molecules

(**A**) BMDMs from WT (black bars) and IRAK2[E525A] (white bars) mice were stimulated with 1.0 μg/ml R848 for the times indicated. RNA was extracted from the cells and *dusp1* and *tnfaip3* mRNA was measured by quantitative real-time PCR. The results are plotted as the fold increase in mRNA relative to the level determined in unstimulated cells. Error bars represent the mean ± SEM for two independent experiments each with BMDMs from three mice of each genotype. (**B**) As in (A), except that BMDMs were stimulated with 1.0 μg/ml Pam_3CSK_4 or 1.0 μg/ml R848 and *il10* mRNA was measured by quantitative PCR. Error bars represent the mean ± SEM for two independent experiments each with BMDMs from three mice of each genotype. (**C**) As in (B), except that the concentration of IL-10 in the cell culture medium was measured. Error bars represent the mean ± SD for two independent experiments each with BMDMs from three mice of each genotype. (**D**) BMDMs from WT (black bars) or IRAK2[E525A] (white bars) mice were incubated for 7 h in the absence of any agonist (control [C]) or stimulated with 1.0 μg/ml R848, 1 μg/ml Pam_3CSK_4 (Pam), 2 μM ODN1826 (CpG-B), 1.0 μg/ml lipoteichoic acid (LTA) or 100 ng/ml LPS (LPS). The concentration of IL-10 in the supernatant was then measured. Error bars represent the mean

± SD for three independent experiments with BMDMs each using three mice of each genotype. *p ≤ 0.05, **p ≤ 0.005, ***p ≤ 0.0005.

Europe PMC Funders Author Manuscripts

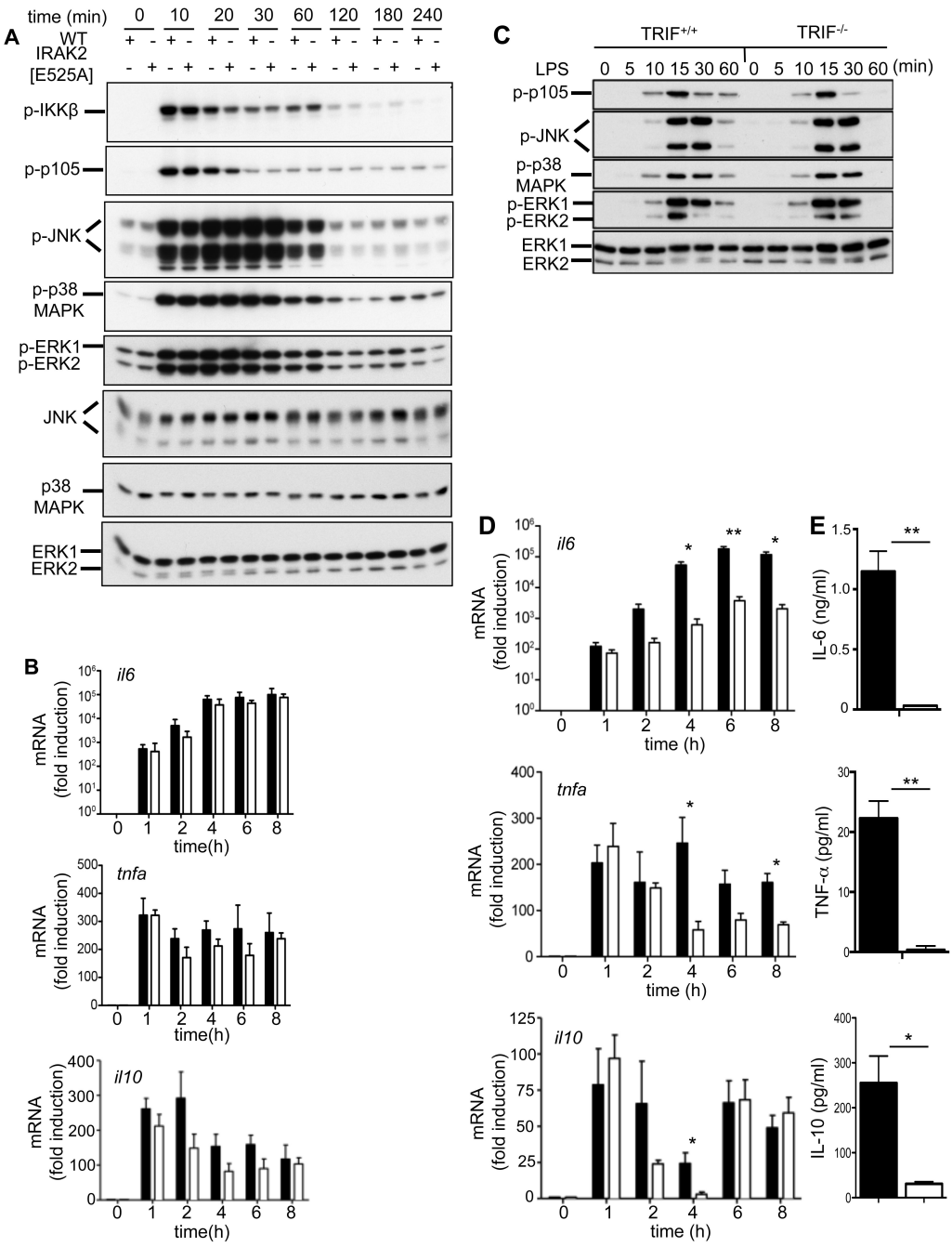

Figure 6. LPS induced protein kinase activation and pro-inflammatory cytokine production in BMDMs from IRAK2[E525A] and TRIF−/− mice

(**A**) Primary BMDMs from WT and IRAK2[E525A] mice were stimulated for the times indicated with 100 ng/ml LPS, and then lysed. Cell extract protein (10 μg) was denatured in SDS, subjected to SDS-PAGE and immunoblotted with the antibodies indicated. The data shown is representative of two independent experiments. (**B**) BMDMs from WT (black bars) and IRAK2[E525A] (white bars) mice were incubated for the times indicated in the presence of 100 ng/ml LPS. RNA was extracted from the cells and *il6*, *tnfa or il10* mRNA was measured by quantitative PCR. The results are plotted as the fold increase in mRNA relative to the level determined in unstimulated cells. Error bars represent the mean ± SEM for

Europe PMC Funders Author Manuscripts

experiments with BMDMs from three mice of each genotype. The data shown is representative of three independent experiments. (**C**) BMDMs from $TRIF^{+/+}$ and $TRIF^{-/-}$ mice were stimulated with 100 ng/ml LPS for the times indicated. Following cell lysis, 20 μg of cell extract protein was denatured in SDS, subjected to SDS-PAGE and immunoblotted with the antibodies indicated. One blot representative of three independent experiments is shown. (**D**) BMDMs from $TRIF^{+/+}$ (black bars) and $TRIF^{-/-}$ (white bars) mice were incubated for the indicated times with 100 ng/ml LPS. RNA was extracted from the cells and *il6* (*upper panel*), *tnfa* (*middle panel*) and *il10* (*lower panel*) mRNA levels were measured by quantitative PCR. The results are plotted as fold increase in mRNA relative to the level determined in unstimulated cells. Error bars represent the mean ± SEM for experiments with BMDMs from three mice of each genotype. The data shown is representative of three independent experiments (**E**) BMDMs from $TRIF^{+/+}$ (black bars) and $TRIF^{-/-}$ (white bars) mice were incubated for 8 h with 100 ng/ml of LPS and the concentrations of IL-6, TNF-α and IL-10 in the cell culture supernatant were measured. The data are representative of two independent experiments with three mice of each genotype analyzed together. Error bars show the mean ± SD. *$p \leq 0.05$, **$p \leq 0.005$).

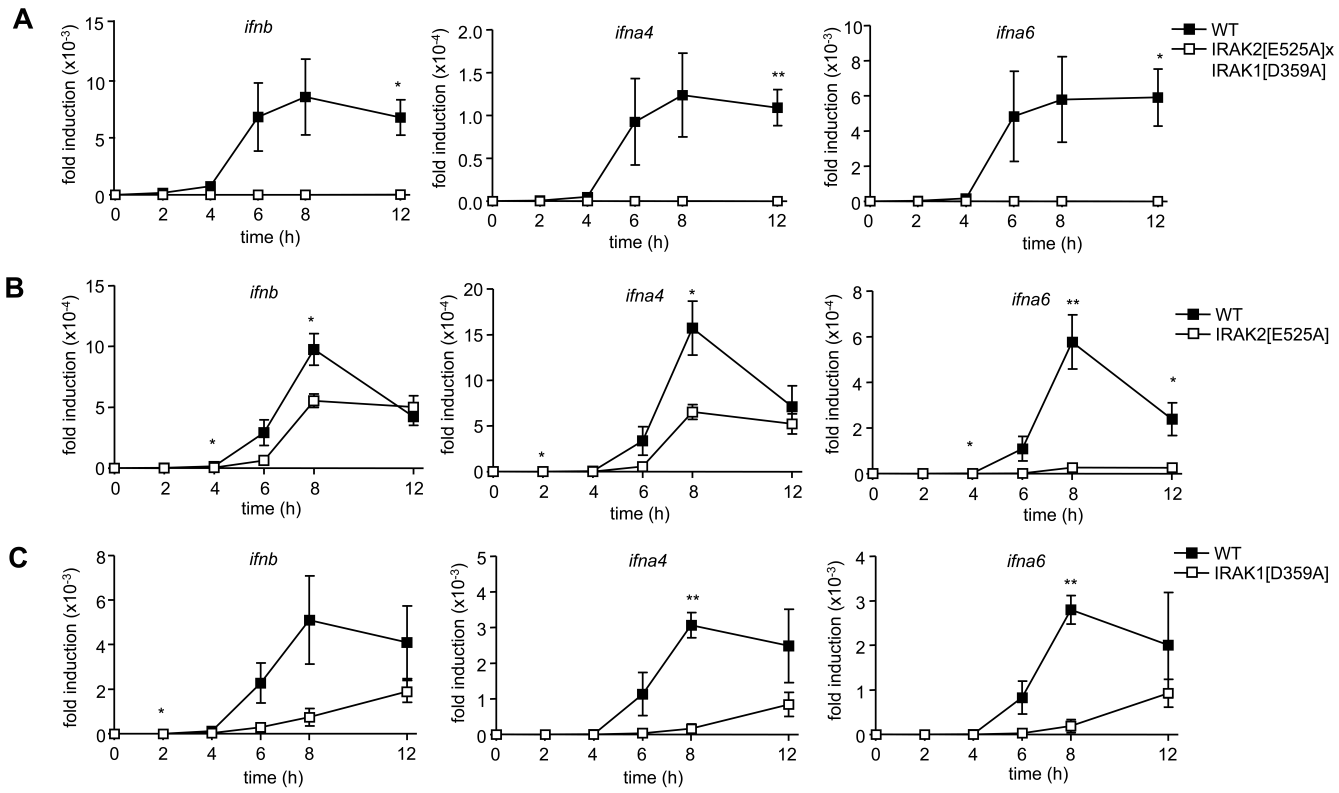

Figure 7. Suppression of type 1 IFN production in pDCs from IRAK2[E525A] mice and IRAK1[D359A] mice

(**A**) pDCs from WT or IRAK2[E525A] × IRAK1[D359A] mice were stimulated for the times indicated with 0.05 μM of CpG B. RNA was extracted from the cells and mRNA encoding *ifnb* (*left panel*), *Ifna4* (*middle panel*) or *Ifna6* (*right panel*) was determined by quantitative PCR. (**B**) As in (A) but pDCs from WT and IRAK2[E525A] mice. (**C**) As in (B) except WT pDCs were compared with IRAK1[D359A] mice. The results are plotted as the fold increase in mRNA relative to the level measured in unstimulated cells. The experiments were performed in 96 well plates with three wells being used for each condition, each containing pDCs from a different mouse. The results are presented as the Mean ± SEM for one representative experiment. Similar results were obtained in two independent experiments. *p ≤ 0.05, **p ≤ 0.005).

Europe PMC Funders Author Manuscripts

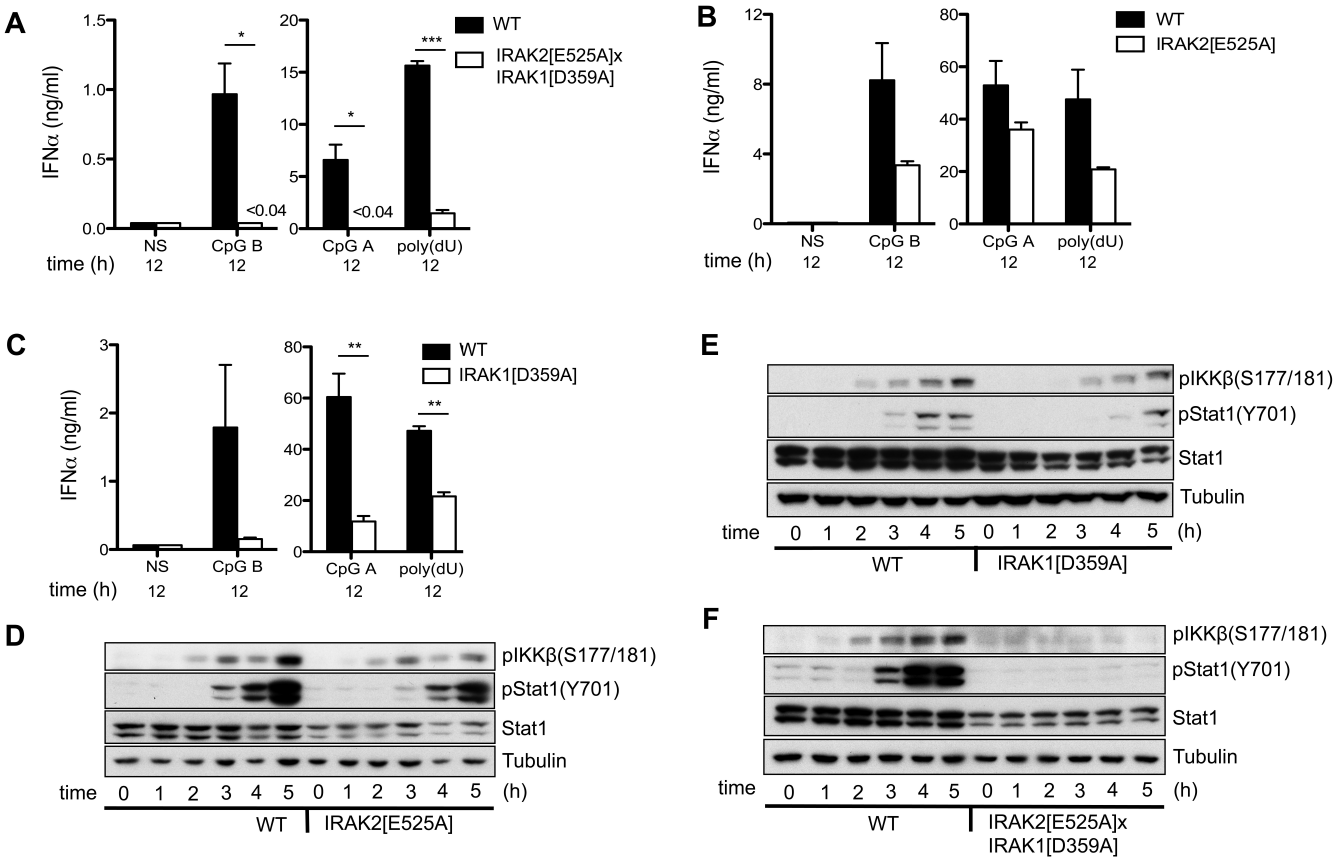

Figure 8. Inhibition on IFN production in IRAK2[E525A] × IRAK1[D359A] mice correlates with impaired activation of IKKβ

(A) pDCs from WT or IRAK2[E525A] × IRAK1[D359A] mice were not stimulated (NS) or stimulated for 12 h with 0.05 μM of CpG B, 1 μM CpG A or 25 μg/ml of poly(dU) and the concentration of IFN-α in the cell culture medium measured by ELISA. (**B**) As in (A) but pDCs from WT or IRAK2[E525A] mice were compared. (**C**) As in (B) except WT pDCs were compared with pDCs from IRAK1[D359A] mice. The experiments were performed in 96 well plates with three wells being used for each condition, each containing pDCs from a different mouse. Bars represent the Mean ± SEM of one representative experiment. (A-C) *p ≤ 0.05, **p ≤ 0.005, ***p ≤ 0.0005. Similar results were obtained in two to three independent experiments. (**D**) pDCs from wild type (WT) or IRAK2[E525A] mice were stimulated for the times indicated with 0.05 μM CpG B and cell lysates subjected to SDS-PAGE followed by immunoblotting with the antibodies indicated. The blot shown is representative of three independent experiments. (**E**) As in (D) except pDCs from wild type (WT) or IRAK1[D359A] were compared. (**F**) As in (E) but pDCs cells from WT and IRAK2[E525A] × IRAK1[D359A] mice were compared. The blots shown are representative of two to three independent experiments.

Europe PMC Funders Author Manuscripts

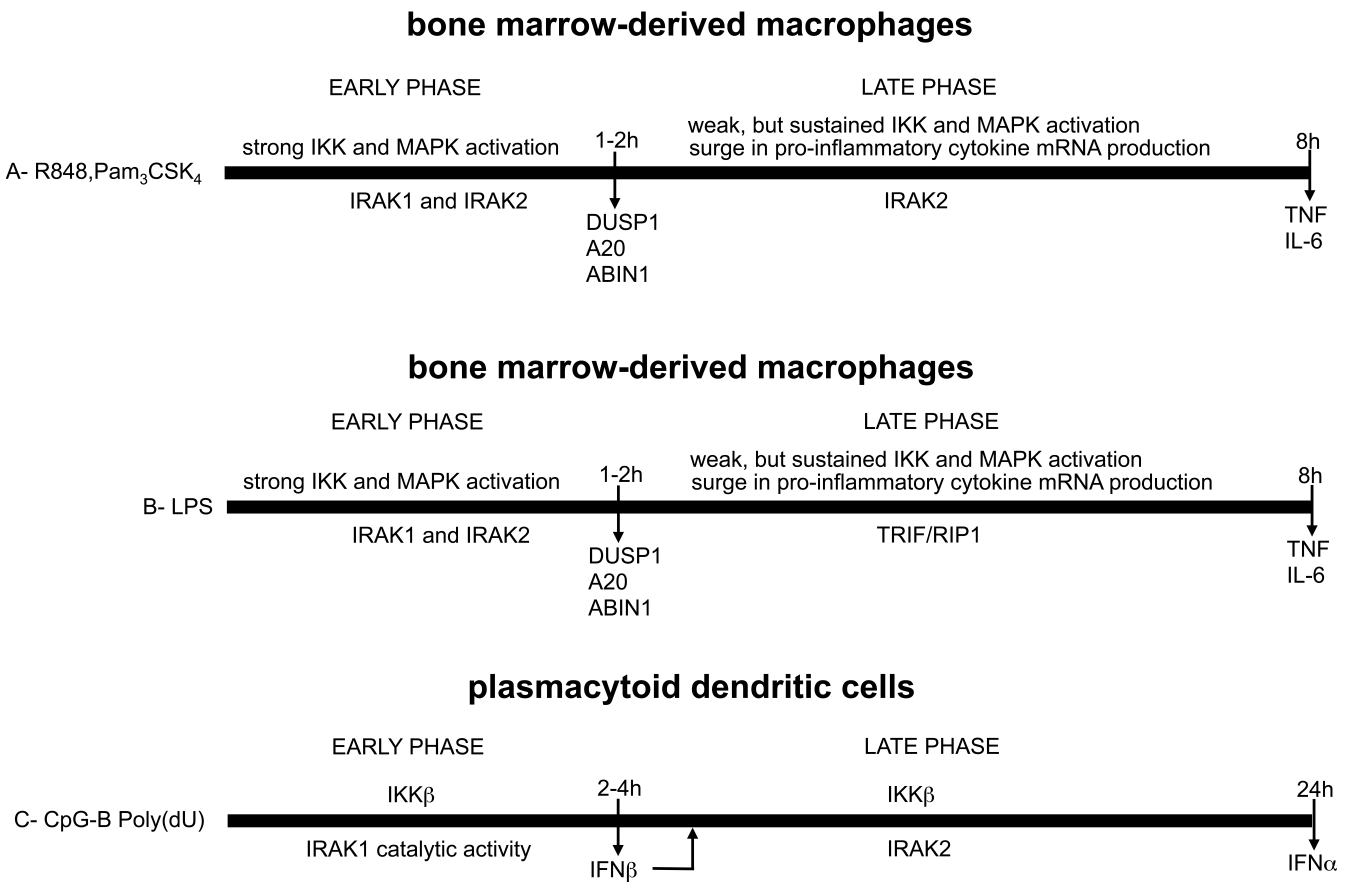

Figure 9. Two phases of inflammatory mediator production defined by the study of IRAK2 and IRAK1 knock-in mice

(**A**) Inflammatory mediator production in BMDMs by TLR agonists that signal via MyD88. (**B**) Inflammatory mediator production in BMDMs by the TLR4 agonist LPS that signals via both MyD88 and TRIF. (**C**) Type 1 IFN production in pDCs by ligands that activate TLR7 and TLR9.